Environ Earth Sci (2017) 76:747
DOI 10.1007/s12665-017-7093-8

ORIGINAL ARTICLE

Geochemical characteristics and controlling factors of chemical composition of groundwater in a part of Guntur district, Andhra Pradesh, India

N. Subba Rao[1] · Deepali Marghade[2] · A. Dinakar[1] · I. Chandana[1] · B. Sunitha[3] · B. Ravindra[1] · T. Balaji[1]

Received: 19 June 2017 / Accepted: 21 October 2017 / Published online: 1 November 2017

Abstract A survey on quality of groundwater was carried out for assessing the geochemical characteristics and controlling factors of chemical composition of groundwater in a part of Guntur district, Andhra Pradesh, India, where the area is underlain by Peninsular Gneissic Complex. The results of the groundwater chemistry show a variation in pH, EC, TDS, Ca^{2+}, Mg^{2+}, Na^{+}, K^{+}, HCO_3^{-}, Cl^{-}, SO_4^{2-}, NO_3^{-} and F^{-}. The chemical composition of groundwater is mainly characterized by Na^{+}–HCO_3^{-} facies. Hydrogeochemical type transits from Na^{+}–Cl^{-}–HCO_3^{-} to Na^{+}–HCO_3^{-}–Cl^{-} along the flow path. Graphical and binary diagrams, correlation coefficients and saturation indices clearly explain that the chemical composition of groundwater is mainly controlled by geogenic processes (rock weathering, mineral dissolution, ion exchange and evaporation) and anthropogenic sources (irrigation return flow, wastewater, agrochemicals and constructional activities). The principal component (PC) analysis transforms the chemical variables into four PCs, which account for 87% of the total variance of the groundwater chemistry. The PC I has high positive loadings of pH, HCO_3^{-}, NO_3^{-}, K^{+}, Mg^{2+} and F^{-}, attributing to mineral weathering and dissolution, and agrochemicals (nitrogen, phosphate and potash fertilizers). The PC II loadings are highly positive for Na^{+}, TDS, Cl^{-} and F^{-}, representing the rock weathering, mineral dissolution, ion exchange, evaporation, irrigation return flow and phosphate fertilizers. The PC III shows high loading of Ca^{2+}, which is caused by mineral weathering and dissolution, and constructional activities. The PC IV has high positive loading of Mg^{2+} and SO_4^{2-}, measuring the mineral weathering and dissolution, and soil amendments. The spatial distribution of PC scores explains that the geogenic processes are the primary contributors and man-made activities are the secondary factors responsible for modifications of groundwater chemistry. Further, geochemical modeling of groundwater also clearly confirms the water–rock interactions with respect to the phases of calcite, dolomite, fluorite, halite, gypsum, K-feldspar, albite and CO_2, which are the prime factors controlling the chemistry of groundwater, while the rate of reaction and intensity are influenced by climate and anthropogenic activities. The study helps as baseline information to assess the sources of factors controlling the chemical composition of groundwater and also in enhancing the groundwater quality management.

Keywords Groundwater · Geogenic processes · Anthropogenic activities · Guntur district · Andhra Pradesh · India

✉ N. Subba Rao
srnandipati@gmail.com

[1] Department of Geology, Andhra University, Visakhapatnam 530 003, India

[2] Priyadarshini Institute of Engineering and Technology, Nagpur 440 001, India

[3] Department of Civil Engineering, JNT University, Hyderabad 500 085, India

Introduction

In developing countries like India, groundwater contamination is a serious problem due to erratic monsoon, rapid growth of population and industrialization, excess usage of agricultural fertilizers and pesticides, lack of adequate soil conservation measures and extraction of groundwater in excess of recharge, which make the stress on aquifer system (Vasanthavigar et al. 2013). By 2050, most parts in

India are likely to face severe water scarcity (SERI 2009). On the other hand, the geogenic processes like anion exchange between F^- and OH^- are responsible for high F^- content in groundwater, cation exchange between Ca^{2+} and Na^+ increases the Na^+ content and evaporation enhances the concentrations of Na^+ and Cl^- in groundwater (Todd 1980; Hem 1991; Drever 1997; Sarikhani et al. 2015). The concentrations of Ca^{2+}, Mg^{2+}, Na^+, K^+, Cl^-, SO_4^{2-}, NO_3^- and F^- also increase in groundwater notably as a result of chemical fertilizers, irrigation return flow, domestic effluents, leakage of septic tanks and constructional activities, which come under non-geogenic origin (Todd 1980; Hem 1991; Somasundaram et al. 1993; Drever 1997; Subba Rao et al. 2005; Ayoob and Gupta 2006; Subba Rao 2008; Jiang et al. 2009; Li et al. 2016). It is also responsible for the higher mineralization (salinity in terms of TDS) in groundwater. Thus, the availability of fresh water is an immense problem everywhere. This is a big constraint not only for drinking, but also for food security in the twenty-first century (Subba Rao 2013).

The assessment of chemical evolution of groundwater is essential, but it is very difficult to find out the contributions of geogenic processes and anthropogenic inputs on the basis of the chemical composition of groundwater alone. The hydrogeochemical facies, graphical analysis, binary diagrams, correlation coefficients, saturation indices and geochemical modeling of groundwater have been widely used to evaluate the chemical characteristics (Piper 1944; Seaber 1962; Back 1966; Li et al. 2010, 2016). However, the multivariate statistical analysis is also widely applied as a tool for understanding the specific hydrogeochemical processes (Dalton and Upchurch 1978; Mahlknecht et al. 2004; Jiang et al. 2009; Nosrati and Eeckhaut 2012; Subba Rao 2014; Marghade et al. 2015). Once the controlling factors of chemical composition of groundwater are established, it is essay to take suitable management measures, accordingly, to improve the groundwater quality.

In recent time, a lot of research work on assessment and protection of groundwater quality has been done in different parts of the world: Senthilkumar et al. (2008) and Srinivasamoorthy et al. (2011) explain the geogenic and anthropogenic sources, which play a key role for variation of chemical composition groundwater in a part of Cuddalore, Tamilnadu, India. Kazi et al. (2009) assess the water quality of polluted lake, using multivariate statistical techniques in Pakistan. Li et al. (2010) elucidate the geochemical modeling of groundwater to explain the water–rock interaction as well as to quantify the evolution processes and the formation mechanisms of the local groundwater chemistry in southern plain area of Pengyang County, Ningxia, China. Nosrati and Eeckhaut (2012) evaluate the groundwater quality, adopting multivariate statistical techniques in Hashtgerd Plain, Iran. Subba Rao et al. (2012a, b) assess the chemical characteristics and assessment of groundwater quality in Gummanampadu sub-basin, Guntur district and Varaha river basin, Visakhapatnam district, Andhra Pradesh, India. Reddy (2013) explains the hydrogeochemical characteristics in groundwater of the southeastern part of Prakasam district, Andhra Pradesh, India. Vasanthavigar et al. (2013) identify the groundwater contamination zones, applying the multivariate statistical approach in Thirumanimuthar sub-basin, Tamil Nadu, India. Singaraja et al. (2014) explain the role of application of statistical analysis of the hydrogeochemical evolution of groundwater in aquifers of Thoothukudi district, Tamil Nadu, India. Marghade et al. (2015) identify the controlling processes of groundwater quality from a Nagpur urban area, Maharashtra, India, using principal component analysis. Sarikhani et al. (2015) assess the hydrochemcial characteristics of groundwater and find that the dissolution of halite resulted in the linear increase in sodium and chloride. The river recharge, dissolution of evaporated minerals and agricultural returned water are responsible for groundwater salinity. Kim and Park (2016) assess the hydrogeochemical characteristics of groundwater in an agricultural area of Hongseong, Korea, adopting multivariate method. Li et al. (2016) evaluate the hydrogeochemical characteristics in an area of irrigated forest of the southeastern edge of the Tengger desert, Northwest China, and find that the salinity in groundwater results from the water–rock interaction, ion exchange, evaporation, irrigated waters and wastewater effluents. Ravikumar and Somashekar (2017) explain the hydrochemical characterizations of groundwater, using principal component analysis, in Varahi river basin, Karnakata, India.

It is essential to evaluate the relationships among the chemical variables and also to identify the local and regional processes, which influence the chemical composition of groundwater. This baseline information plays a significant role for the establishment of long-term groundwater monitoring programs for sustainable development of an area. The hydrogeochemical facies, graphical analysis, binary diagrams, correlation coefficients, saturation indices and geochemical modeling of groundwater are used in this study. In addition, the multivariate statistical analysis is also used to identify the variation of groundwater chemistry through data reduction and classification and also helps to simplify and organize the data set in order to make useful generalizations and insight into water systems. Therefore, the purpose of this study is (1) to investigate the geochemical characteristics of groundwater and (2) to determine the factors controlling the groundwater chemistry. This research will be helpful in enhancing the groundwater quality management.

Study area

The Sattenapalle area is located in Guntur district, Andhra Pradesh, India (Fig. 1). It covers an area of about 235 km^2, falling in the Survey of India toposheet 65 D/3. The area comes under semiarid climatic region with an average air temperature of 25 °C in winter (December and February) to 46 °C in summer (March and May). The annual rainfall over the study area is 750 mm (CGWB 2013). Most of it (63%) receives from southwest monsoon (June to September). About 27% of the total rainfall is contributed by northeast monsoon (October to December). The rest (10%) comes from the remaining period.

Topographically, the highest contour elevation is 80 m above mean sea level (amsl) at southwestern side and the lowest is 60 m amsl at northern and eastern sides (Fig. 2). The sloping of the area, thus, follows the topographical features. As a result, the streams flow toward northern and eastern sides from southwestern side (Fig. 3). Drainage pattern shows sub-dendritic type. Streams flow only during monsoon. The black cotton soil is the dominated type. The calcium carbonate concretions (locally known as *kankar*) occur in the soil zone, which is a characteristic feature of the semiarid climate. Geologically, the entire study area is underlain by rocks of banded–biotite–hornblende gneisses with migmatite patches of the Peninsular Gneissic Complex (CGWB 2013). They contain the quartz, plagioclase and orthoclase feldspars, biotite, hornblende and apatite minerals. Dolerite and pegmatite occur as intrusive bodies. The rocks show a strike of NE–SW with a dip of 45°SE.

The rocks of the Peninsular Gneissic Complex are the predominant water-bearing formations with lack of primary porosity. The occurrence of groundwater depends upon the secondary porosity developed by weathering processes and fracturing activities of the rocks. As per the well owner's information, the depth of top soil varies from 2 to 3 m from the ground surface, the weathering rock portion from 2 to 16 m, which is characterized by low hydraulic conductivity, and the rock fractured zone from 14 to 68 m, which is represented by high hydraulic conductivity. The clay products, resulting from the highly weathering activity in the upper part of the bedrock, reduce the hydraulic conductivity to some extent. Generalized design of dug well and bore well is shown in Fig. 4.

Groundwater is extracted through dug wells and bore wells. The former wells are mainly confined to the weathered zone under unconfined conditions, while the latter wells extend into the fractured zone under semi-confined conditions. According to the information of well owners, the depth of bore wells varies from 45 to 65 m below ground level (bgl). During drilling, the water is struck at a depth of 10–15 m bgl. The depth to water levels varies from 3 to 5 m bgl. The yield of bore wells, in general, varies between 1 and 5 L per second (CGWB 2013).

Rainfall is the main direct recharge, and irrigation water is the indirect recharge source of the groundwater. Most of the people depend on agriculture as a profession. Irrigation is intensive and long-term practice, using both surface water and groundwater. Because of the brackish type of groundwater, it is mostly used for irrigation. Application of soil amendments, agricultural fertilizers and pesticides is a common phenomenon. Drainage conditions are poor. Constructional activities are not uncommon. Important crops are rice, chilies and grains.

Materials and methods

Sample collection and chemical analysis of groundwater

For the assessment of geochemical characteristics and controlling factors of groundwater chemistry as a baseline information, a groundwater quality survey was conducted in the present study area during summer (May) 2014 and collected 20 groundwater samples from bore wells (Fig. 1), which extent up to a depth of semi-confined aquifer. Prior to groundwater sampling, all wells were pumped for several minutes to eliminate the influence from stagnant water. Groundwater samples were collected in 500-mL polyethylene bottles, which had been rinsed and washed 3–4 times, using water to be sampled. After sampling, the groundwater samples were labeled, stored and transported to the laboratory for chemical analysis.

The groundwater samples were analyzed for hydrogen ion concentration (pH), electrical conductivity (EC), total dissolved solids (TDS), calcium (Ca^{2+}), magnesium (Mg^{2+}), sodium (Na^{+}), potassium (K^{+}), bicarbonate (HCO_3^{-}), chloride (Cl^{-}), sulfate (SO_4^{2-}), nitrate (NO_3^{-}) and fluoride (F^{-}), following the procedures of American Public Health Association (APHA 1992). The pH and EC were measured in the field, using their portable meters. The EC was used to calculate the concentration of TDS, as per the suggestion of Hem (1991). The TH (as $CaCO_3$) and Ca^{2+} were estimated by EDTA titration method. The concentration of Mg^{2+} was computed, taking the difference TH and Ca^{2+}. A flame photometer was used for the estimation of Na^{+} and K^{+} ions. The HCO_3^{-} was measured by HCl volumetric method. The Cl^{-} was analyzed by $AgNO_3$ titration method. The SO_4^{2-} was determined, using turbidimetric procedure, also the NO_3^{-}, using colorimetric method and the F^{-}, using specific ion analyzer. The units of EC are expressed in microsiemens per centimeter (μS/cm) at 25 °C and the remaining chemical variables (except pH) in milligrams per liter (mg/L).

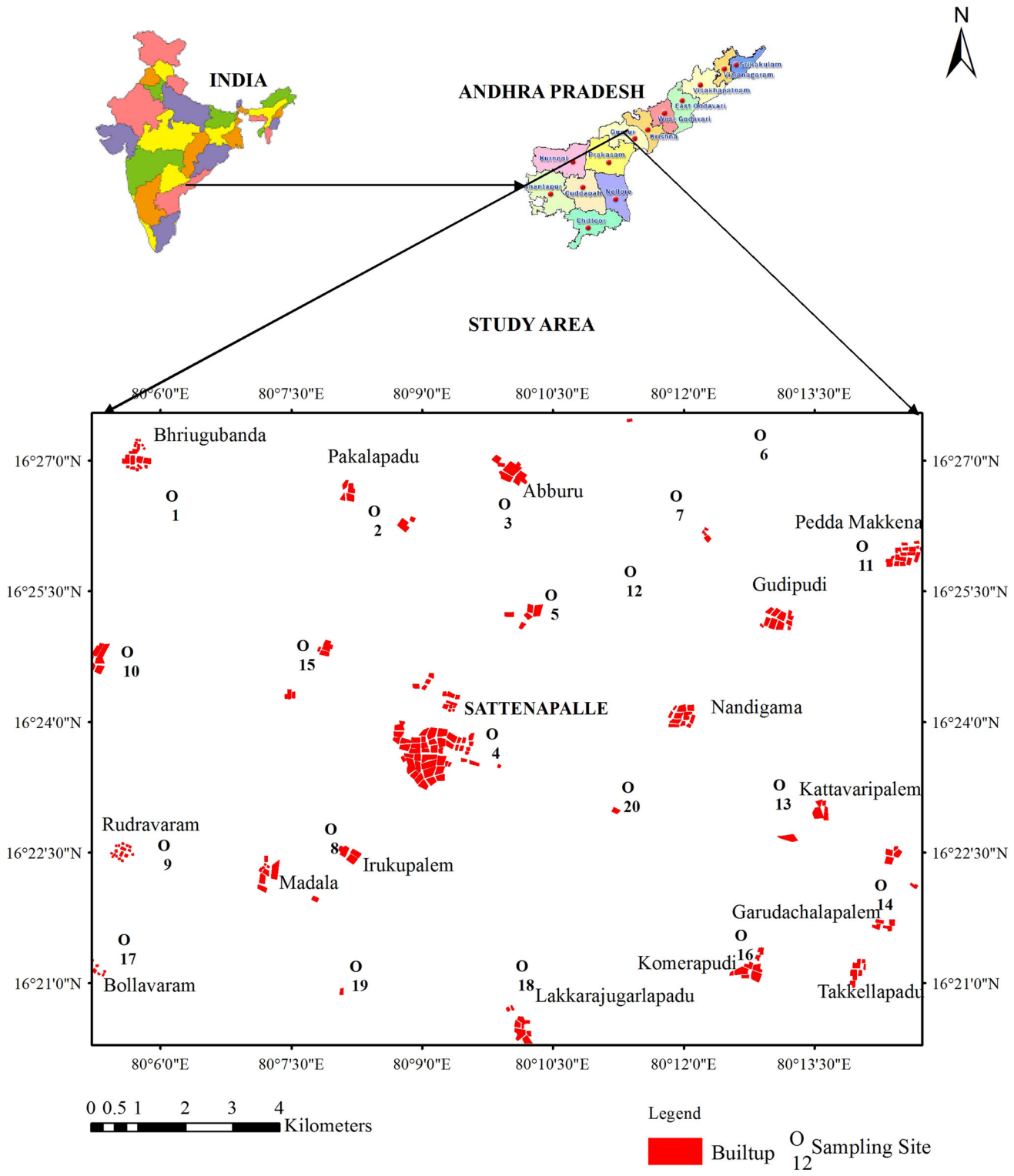

Fig. 1 Location of the study area and sampling sites

For analytical accuracy between the concentrations of total cations (Ca^{2+}, Mg^{2+}, Na^{+} and K^{+}) and the concentrations of total anions (HCO_3^{-}, Cl^{-}, SO_4^{2-}, NO_3^{-} and F^{-}) expressed in milliequivalent per liter (meq/L) of the each sample, ionic balance error (IBE) was computed (Eq. 1). This was observed to be within the acceptable limit of ± 5% (Domenico and Schwartz 1990).

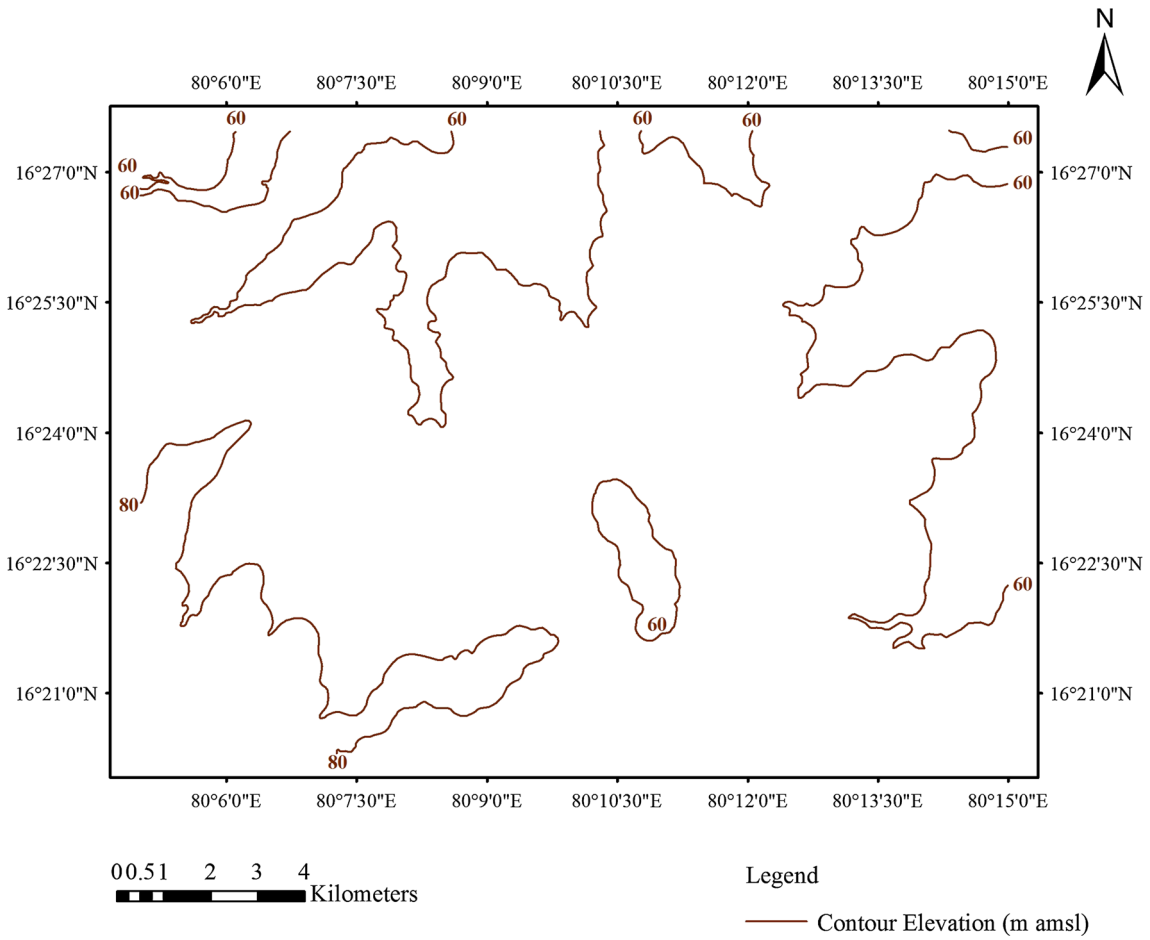

Fig. 2 Contour elevation

$$\text{IBE} = \frac{\sum \text{Cations} - \sum \text{Anions}}{\sum \text{Cations} + \sum \text{Anions}} \times 100 \quad (1)$$

Statistical analysis

STATISTICA software (version 6) was used here to describe how much data set vary and allow using statistics to compare the data to other sets of data. It is expressed in four ways: (a) central tendency (arithmetic mean), (b) dispersion (standard deviation), (c) relative standard deviation (coefficient of variance) and (d) degree of association among chemical variables (correlation coefficient). The respective formulae are shown below (Eqs. 2–5).

$$\text{Arithmetic mean } (\bar{x}) = \frac{\sum x_i}{n} \quad (2)$$

$$\text{Standard deviation } (\sigma) = \sqrt{\sum \frac{(x_i - \bar{x})^2}{df}} \quad (3)$$

$$\text{Correlation coefficient } (r) = \frac{\sum (x_i - \bar{x})(y_i - \overline{y_i})}{n \cdot \sigma_x \cdot \sigma_y} \quad (4)$$

$$\text{Coefficient of variation (CV)} = \frac{\sigma}{\bar{x}} \times 100 \quad (5)$$

where x_i is random variable, n is total number of observations, df is degree of freedom, y_i is other random variable, σ_x is standard deviation of x_i and σ_y is standard deviation of y_i.

Here also, STATISTICA software (version 6) was used to know the relative variation of chemical variables influencing the chemical composition of groundwater. Thus, the chemical variables were expressed in box plots, which characterize a sample in terms of median, range and shape of the data distribution, using 25th, 50th and 75th percentiles.

The multivariate statistical analysis was performed, using STATISTICA software (version 6), to reduce and organize large data sets into groups with similar characteristics. The 11 chemical variables (pH, TDS, Ca^{2+}, Mg^{2+}, Na^{+}, K^{+}, HCO_3^{-}, Cl^{-}, SO_4^{2-}, NO_3^{-} and F^{-}) were used for the principal component analysis. Varimax

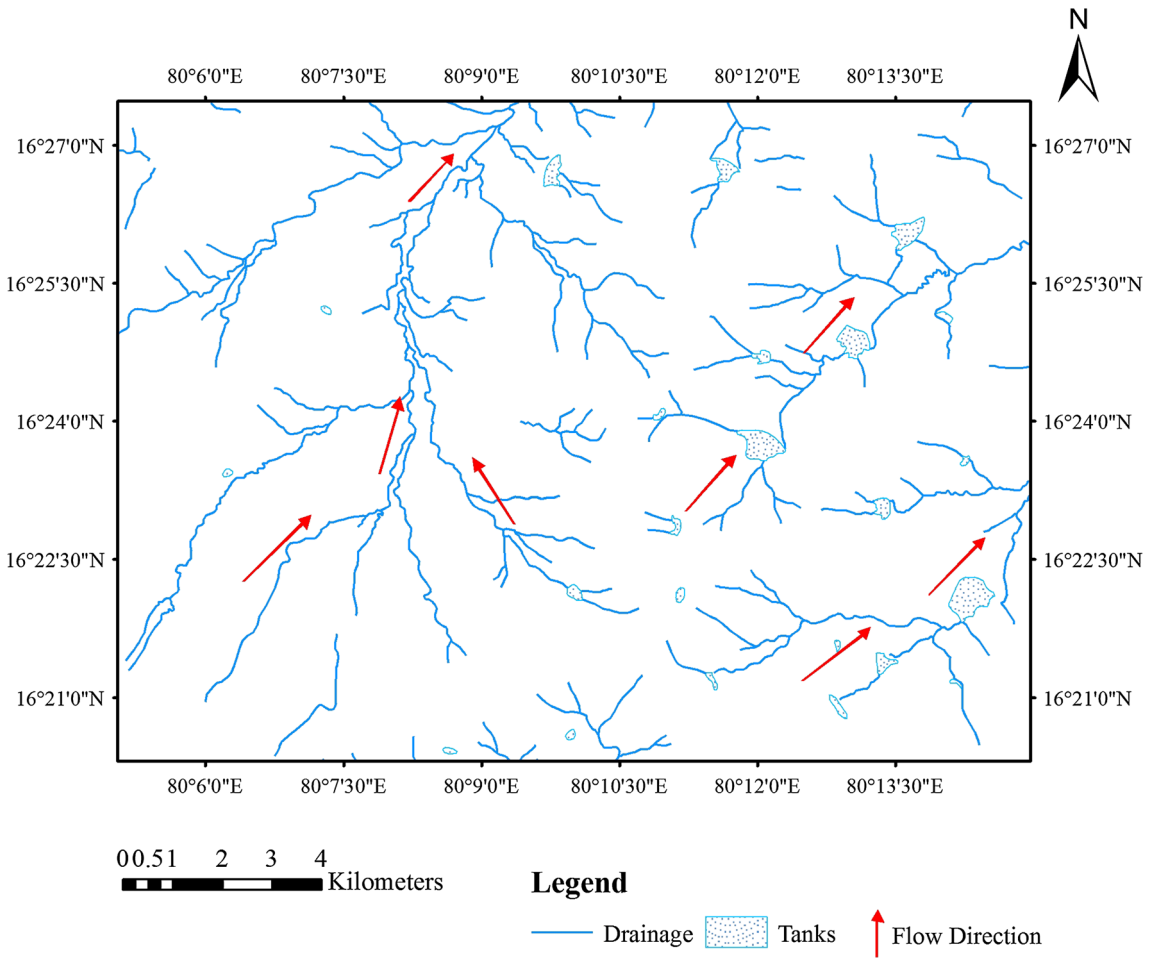

Fig. 3 Drainage and flow direction

rotation was applied here to increase the participation of the chemical variables with higher contribution and reduce those with lesser contributions (Davis 1986). Kaiser's criterion of principal components with eigenvalue more than one was taken into consideration (Kaiser 1958). The first principal component is related to the largest eigenvalue, which explains the greatest amount of variance in the data set. The second principal component, which is orthogonal and uncorrelated with the first one, explains most of the remaining variance and so forth. The Pearson correlation coefficient matrix of the raw data (20 groundwater samples × 11 chemical variables) was computed.

Hydrogeochemical facies

The concept of hydrogeochemical facies has been widely used to explain the distribution and genesis of principal groundwater types along the water flow path (Seaber 1962; Back 1966; Subba Rao et al. 2012a). The facies were classified by taking the ionic percentages in the relative decreasing order of their abundances and neglecting the less than 5% of the total concentration of ions as insignificant (Khan et al. 1972).

Saturation indices and geochemical modeling of groundwater

In the hydrogeochemical study, the PHREEQC software, a thermodynamic program (Parkhurst and Appelo 1999), was used to calculate saturation index (SI) and to perform the inverse geochemical modeling or for understanding the hydrochemical evolution mechanisms (Li et al. 2010). The intensity of soluble minerals expressed in terms of saturation index (SI) has been widely used to evaluate the degree of equilibrium between water and respective mineral (Eq. 6).

$$\mathrm{SI} = \frac{K_{\mathrm{IAP}}}{K_{\mathrm{SP}}} \tag{6}$$

where IAP is the ion activity product and SP is the solubility product.

If SI is more than zero, it indicates oversaturation (precipitation) with respect to the particular mineral. If SI

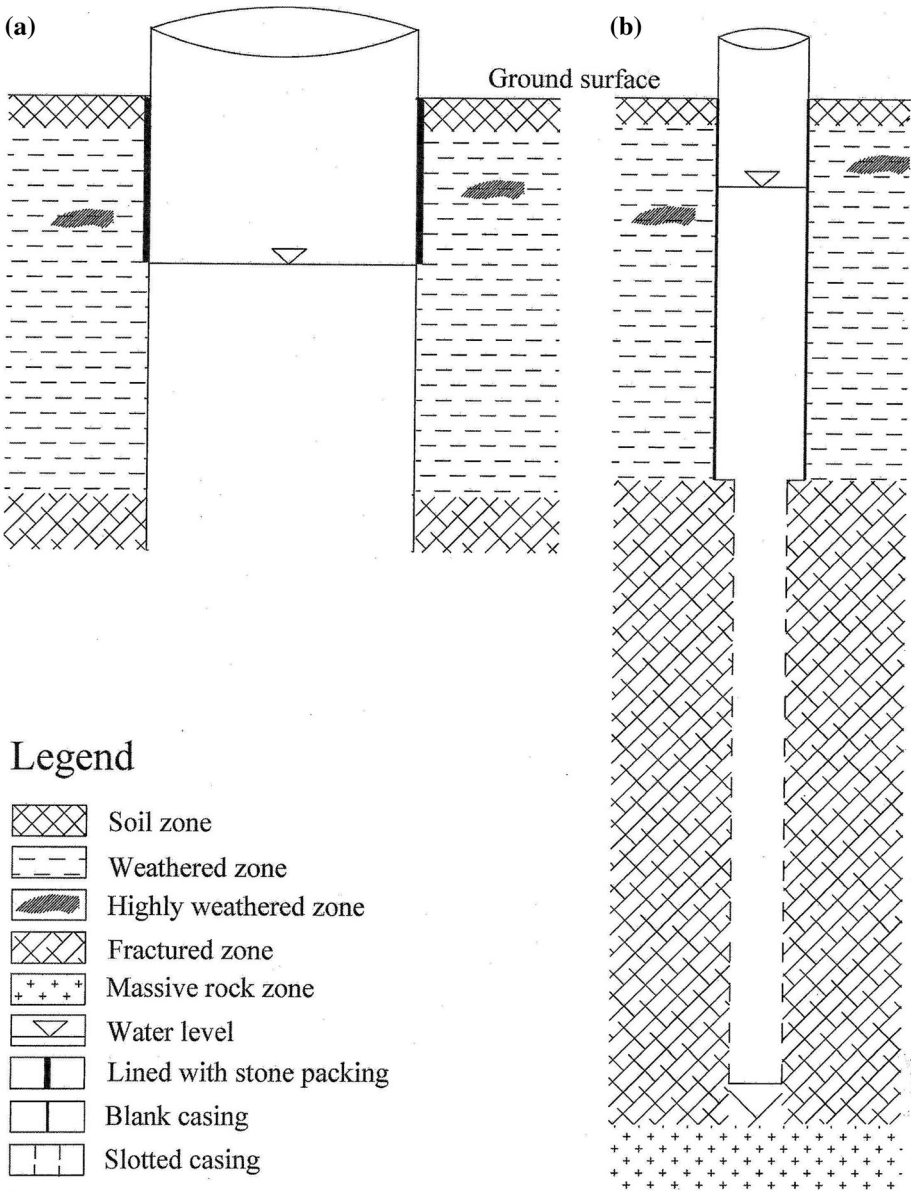

Fig. 4 Generalized design of **a** dug well and **b** bore well

is less than zero, it means undersaturation (dissolution) with respect to the concerned mineral. If SI is equal to zero, it suggests saturation (equilibrium) with respect to the particular mineral solution.

Geochemical modeling is an important tool for studying the hydrogeochemical evolution of mechanisms (Li et al. 2010, 2016). Inverse geochemical modeling, which determines the amount of dissolved or deposited minerals and gases at two points along the groundwater flow line, is mainly used to study chemical reactions taking place along the groundwater flow line to calculate the moles of minerals and gases that have dissolved in or precipitated/degassed to explain the differences in composition between the initial and final end member solutions (Li et al. 2016). The mass balance of the conceptual models is expressed as follows:

$$\sum_{j=i}^{n} a_{ij} x_j = b_i \tag{7}$$

where a_{ij} is the stoichiometric number of element i in mineral j, x_j is the molar number of minerals or gases that have dissolved or precipitated (degassed) and b_i is the increment of element i in the final water solution compared with the initial water solution (Li et al. 2010, 2016). Positive values of mass transfer indicate dissolution of minerals or gas, while negative values indicate precipitation or outgassing.

Results and discussion

Groundwater quality

Table 1 shows the results of the chemical composition of groundwater of the study area (Fig. 1). They are compared with the standard drinking water limits of WHO (2011) and BIS (2012). The pH is from 7.1 to 8.8 (mean 7.89), which is within the highest desirable limit of 6.5–8.5 prescribed for drinking, indicating an alkaline condition of groundwater. The EC, which is from 2090 to 3367 µS/cm (mean 2835.75 µS/cm), reflects the amount of material dissolved in the groundwater. As per the classification of EC (Subba Rao et al. 2012b), 80% of the total groundwater samples come under type II (medium enrichment of salts) and the rest (20%) belong to type III (high enrichment of salts). The TDS varies from 1360 and 2190 mg/L (mean 1823.75 mg/L), which indicates a wide variation in the degree of water salinity due to involvement of various factors responsible for chemical composition of groundwater. The values of TDS are above the safe limit of 500 mg/L allowed for drinking in all groundwater samples, which may cause an inferior palatability and gastrointestinal irritation.

The Ca^{2+} is in between 50 and 90 mg/L (mean 68 mg/L) and the Mg^{2+} from 42 to 95 mg/L (mean 70.25 mg/L, Table 1). Their contributions to the total ionic concentrations are 11.87 and 20.24%, respectively. In 35% of the total groundwater samples, the Ca^{2+} is more than the desirable limit of 75 mg/L recommended for drinking water. The Mg^{2+} is higher than that of its desirable limit of 30 mg/L prescribed for drinking water in all groundwater samples. Both of these ions lead to a scale formation on water distribution structures. The Na^{+} ranges from 235 to 546 mg/L (mean 402.55 mg/L), and its contribution is 61.31% to the total cationic concentration. The concentration of Na^{+} is more than the allowable limit of 200 mg/L suggested for drinking use. It may cause hypertension. The K^{+} is from 35 to 89 mg/L (mean 61.80 mg/L), which contributes to the total ionic concentration of 6.58%.

Table 1 Chemical composition of groundwater

Sample No.	pH	EC (µS/cm)	TDS (mg/L)	Ca^{2+} (mg/L)	Mg^{2+} (mg/L)	Na^{+} (mg/L)	K^{+} (mg/L)	HCO_3^{-} (mg/L)	Cl^{-} (mg/L)	SO_4^{2-} (mg/L)	NO_3^{-} (mg/L)	F^{-} (mg/L)
1	7.2	2880	1480	60	50	479	35	475	665	77	30	1.3
2	7.9	2832	1840	80	58	410	65	855	420	80	47	1.8
3	7.6	2582	1680	90	42	373	60	785	360	89	61	1.6
4	7.6	3060	1990	50	92	442	51	900	420	150	51	1.5
5	8.1	2910	1890	70	88	370	66	810	445	141	51	1.9
6	7.9	2903	1885	70	85	385	57	875	445	73	53	1.7
7	7.8	2090	1360	50	80	235	53	795	225	36	57	1.7
8	7.1	2862	1860	50	56	469	45	600	560	112	34	1.3
9	8.0	2753	1790	80	73	370	67	825	410	54	59	1.9
10	8.3	2930	1905	80	95	347	84	865	445	75	70	2.6
11	7.3	2955	1920	70	50	478	45	635	550	130	50	1.5
12	8.4	2928	1900	80	90	354	88	835	425	117	78	2.8
13	7.9	2306	1500	50	80	290	59	670	355	45	55	1.7
14	8.4	2961	1925	60	52	461	89	870	445	67	78	2.9
15	8.8	3367	2190	50	74	546	53	1055	470	65	65	12.9
16	7.3	3029	1970	70	65	460	45	590	665	75	32	1.4
17	8.4	3052	1985	80	85	395	75	850	475	110	74	2.6
18	8.2	2948	1915	60	85	402	72	810	440	130	70	2.3
19	7.8	2700	1755	70	55	405	64	790	390	90	51	1.8
20	7.7	2667	1735	90	50	380	63	760	400	92	53	1.7
M	7.89	2835.75	1823.75	68.00	70.25	402.55	61.80	782.50	450.50	90.40	55.95	2.45
SD	0.46	275.69	196.23	13.61	17.21	70.68	14.74	131.19	100.95	31.97	14.04	2.51
CV (%)	5.83	9.72	10.76	20.01	24.50	17.56	24.05	16.77	22.41	35.37	25.09	102.45
IC (%)	–	–	–	11.87	20.24	61.31	6.58	45.10	44.62	6.61	3.22	0.45
DWQS	6.5–8.5	–	500	75	30	200		300	250	150	45	1.5

M mean, *SD* standard deviation, *CV* coefficient of variation, *IC* ionic contribution, *DWQS* drinking water quality standards (WHO 2011; BIS 2012)

The HCO_3^- is from 475 to 1055 mg/L (mean 782.50 mg/L), and its contribution to the total anionic concentration is 45.10% (Table 1). The concentration of HCO_3^- is higher than the desirable limit of 300 mg/L in all groundwater samples. The Cl^- varies from 225 to 665 mg/L (mean 450.50 mg/L), which contributes to the total ionic concentration of 44.62%. The Cl^- content is more than the threshold limit of 250 mg/L in 95% of the total groundwater samples, which may cause salty taste. The SO_4^{2-} is in between 36 and 150 mg/L (mean 90.40 mg/L), which contributes 6.61% to the total anions. This is within the safe limit of 150 mg/L recommended for drinking in all groundwater samples. The NO_3^- is from 30 to 78 mg/L (mean 55.95 mg/L). The contribution of NO_3^- is 3.22% to the total anions. The safe limit of NO_3^- for drinking water is 45 mg/L. In 85% of the total groundwater samples, it exceeds its safe limit, which may cause blue baby disease. The F^- varies from 1.3 to 12.9 mg/L (mean 2.45 mg/L), which contributes 0.45% to the total anions. In 75% of the total groundwater samples, the content of F^- is more than its desirable limit (1.5 mg/L) prescribed for drinking water, which may cause fluorosis.

Statistical variability

From Table 1, it is significant to note that there is a lot of differences in the values of standard deviation (0.46–275.69), indicating a wide dispersion of salts in the groundwater system due to involvement of various hydrogeochemical processes. This is also clearly reflected in the values of coefficient of variation. For examples, the F^- shows the highest coefficient of variation (102.45%) and pH the lowest coefficient of variation (5.83%). Nitrate (25.09%), Mg^{2+} (24.50%) and K^+ (24.05%) have almost the same values of coefficient of variation. Similarly, Na^+ (17.56%) and HCO_3^- (16.77%) as well as TDS (10.76%) and EC (9.72%) show almost the same values of coefficient of variation. Sulfate (35.37%) and Cl^- (22.41%) have the different values of coefficient of variation. The difference in the values of coefficient of variation among the chemical variables clearly reflects the spatial variation of chemical composition of groundwater.

Box plots

Box plots are used here to identify the chemical variables, which relatively influence the groundwater chemistry. They show the median, range and shape of the data distribution (Fig. 5). The median (small square), lower and upper quartile (big square—25–75%), non-outlier range (vertical line with bottom and upper line), outlier value (round) and extreme value (star) represent the relative variation of chemical variables within the groundwater chemistry. The box plots of the chemical composition show that the EC, TDS, Na^+, HCO_3^- and Cl^- have the largest variability and the remaining (pH, Ca^{2+}, Mg^{2+}, K^+, SO_4^{2-}, NO_3^- and F^-) the smallest variability. These clearly suggest that the local contamination inputs play a major role over the regional processes controlling the groundwater chemistry.

Hydrogeochemical analysis

Hydrogeochemical analysis is discussed in terms of hydrogeochemical evolution, hydrogeochemical facies, geochemistry of groundwater along the flow path and controlling processes of geochemistry of groundwater. The principal component analysis is used to assess the relative influencing factors on the chemical composition of groundwater. Geochemical modeling of groundwater is also used for supporting the findings observed from the hydrogeochemical analysis.

Hydrogeochemical evolution

A trilinear diagram (Fig. 6) is used here for characterization of hydrogeochemical evolution (Piper 1944). The diagram has two triangles and one diamond-shaped field: First triangle is related to cations on left side, second one to anions on right side, which are in the lower side, and third one is on the upper side, which is above these two triangles, to plot an overall chemical composition of groundwater for the characterization of hydrogeochemical evolution through assessment of various water types, viz. zone 5 ($CaHCO_3$ type), zone 6 (CaCl type), zone 7 (NaCl type), zones 8 ($NaHCO_3$ type) and 9 (mixed type or transition type).

As shown in Fig. 6, 10% of the total groundwater sampling points (19) fall in zone 5, 50% of the groundwater sampling points (1, 2, 5, 8, 10, 11, 13, 16, 17 and 20) in zone 7 and the rest (45%) of the groundwater sampling points (3, 4, 6, 7, 9, 12, 14, 15, 18 and 19) in zone 9. It suggests that the fresh water (zone 5) moves toward the saline water (zone 7) through the mixed water (zone 9) due to influence of anthropogenic activity on the groundwater quality.

Hydrogeochemical facies

Groundwater flows from the upstream to the downstream, which is a natural phenomenon. During this way, water–rock interactions can occur, thereby naturally increasing the ionic concentrations in groundwater (Todd 1980; Hem 1991). In addition, ionic concentrations can also increase by anthropogenic activities (Subba Rao 2002; Subba Rao et al. 2012a; Li et al. 2016). Therefore, it is essential for

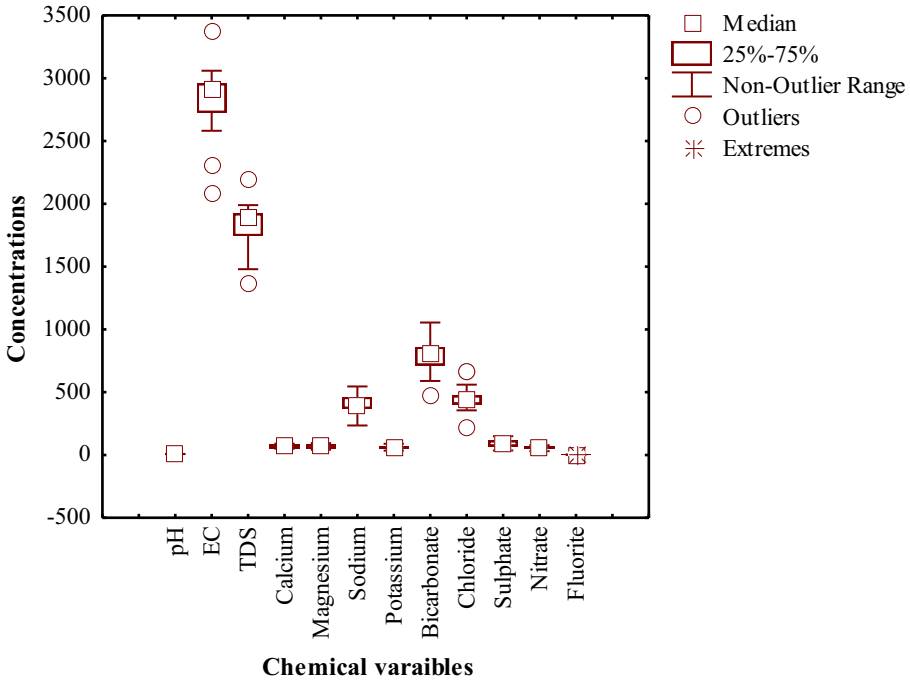

Fig. 5 Box plots

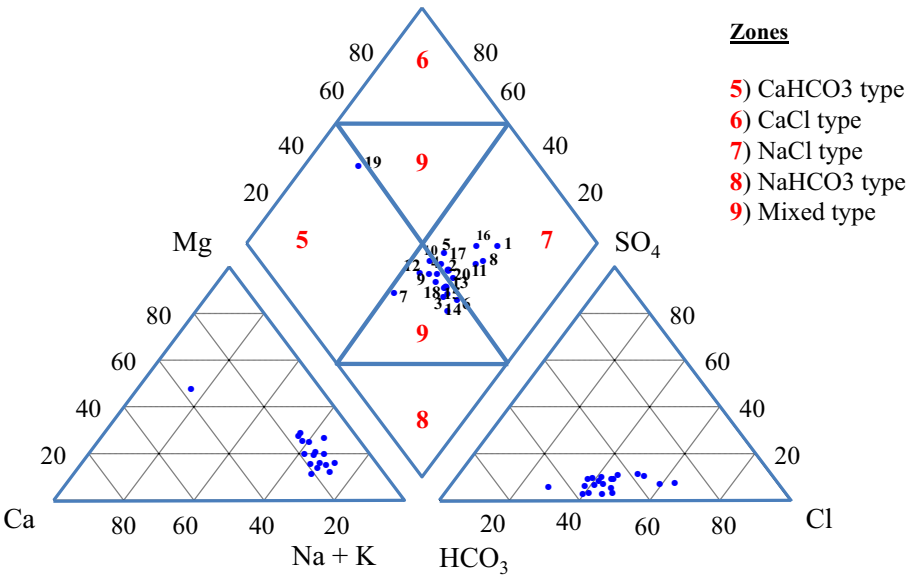

Fig. 6 Trilinear diagram (after Piper 1944)

understating the role of sources of natural and artificial origins on the aquifer chemistry, following the flow path. In the present study area, five types of the hydrogeochemical facies are observed (Table 2). They are (a) $Na^+ > Mg^{2+} > Ca^{2+} > K^+$: $HCO_3^- > Cl^- > SO_4^{2-}$ (b) $Na^+ > Mg^{2+} > Ca^{2+}$: $HCO_3^- > Cl^- > SO_4^{2-}$, (c) $Na^+ > Mg^{2+} > Ca^{2+} > K^+$: $HCO_3^- > Cl^-$, (d) $Na^+ > Mg^{2+} > Ca^{2+}$: $Cl^- > HCO_3^- > SO_4^{2-}$ and (e) $Na^+ > Mg^{2+} > Ca^{2+}$: $HCO_3^- > Cl^-$.

Fifty percent groundwater samples are represented by $Na^+ > Mg^{2+} > Ca^{2+} > K^+$: $HCO_3^- > Cl^- > SO_4^{2-}$ facies (Table 2). Twenty percent of the groundwater samples are characterized by two types of facies, which are $Na^+ > Mg^{2+} > Ca^{2+} > K^+$: $HCO_3^- > Cl^-$ and $Na^+ > Mg^{2+} > Ca^{2+}$: $Cl^- > HCO_3^- > SO_4^{2-}$. Similarly, 5% of the groundwater samples are characterized by two types of facies, which are $Na^+ > Mg^{2+} > Ca^{2+}$: $Cl^- > HCO_3^- > SO_4^{2-}$ and $Na^+ > Mg^{2+} > Ca^{2+}$: $HCO_3^- > Cl^-$. As a whole on the basis of dominant ions among cations and anions, the hydrogeochemical facies are characterized by Na^+–HCO_3^- and Na^+–Cl^- types in 80% and 20% of the total groundwater samples, respectively.

Table 2 Hydrogeochemical facies

Hydrogeochemical facies	Samples	
	Numbers	Percentage
$Na^+ > Mg^{2+} > Ca^{2+}$: $HCO_3^- > Cl^-$	15	5
$Na^+ > Mg^{2+} > Ca^{2+}$: $HCO_3^- > Cl^- > SO_4^{2-}$	4	5
$Na^+ > Mg^{2+} > Ca^{2+} > K^+$: $HCO_3^- > Cl^-$	7, 9, 13 and 14	20
$Na^+ > Mg^{2+} > Ca^{2+} > K^+$: $HCO_3^- > Cl^- > SO_4^{2-}$	2, 3, 5, 6, 10, 12, 17 and 20	50
$Na^+ > Mg^{2+} > Ca^{2+}$: $Cl^- > HCO_3^- > SO_4^{2-}$	1, 8, 11 and 16	20

It is noted that all groundwater samples show commonly the $Na^+ > Mg^{2+} > Ca^{2+}$ facies among cations (Table 2). However, 70% of the total groundwater samples show the K^+ ion, which is in addition to the common cation-related facies. Further, it is also significant to note that the 80% of the groundwater samples have the $HCO_3^- > Cl^-$ facies, while the 20% of the groundwater samples show the $Cl^- > HCO_3^-$ facies. Here also, 75% of the total groundwater samples are shown by SO_4^{2-} as the additional ion in their anion facies. Therefore, the K^+ and SO_4^{2-} are the additional contributions of ions to the common facies. This is a result of anthropogenic influence on the aquifer chemistry. Otherwise, all groundwater samples should have the same facies. Therefore, the differences in the distribution of ions, following the flow path, clearly suggest the enrichment of chemical composition of groundwater due to interference of human activities over the geochemistry of groundwater of geogenic origin.

Groundwater chemistry along the flow path

To have more clarification on assessment of the variation of chemical composition along the specific flow path, two representative flow paths (from 8 to 2 and from 16 to 14) are selected (Figs. 1, 2, 3), according to the topographical, drainage and hydrogeological conditions. It reflects the changes in groundwater chemistry from the upstream to the downstream. In the first flow path, the sampling site 8 is relatively at the upstream and 2 is at the downstream on left side, where the traveling distance of the groundwater between the sampling sites is about 8 km. In the second flow path, the sampling site 16 is comparatively at the upstream and 14 is at the downstream on right side, where the traveling distance of the groundwater between the sampling sites is about 3 km. In all groundwater samples, Na^+ is the dominant ion among cations, while HCO_3^- and Cl^- are the dominant ions among anions in 80% and 20% of the total groundwater samples, respectively (Table 2). Thus, these three ions are taken into consideration to evaluate the variation in chemical composition of groundwater along the flow paths.

In the upstream side, the groundwater shows the Na^+–Cl^-–HCO_3^- type, while it has Na^+–HCO_3^-–Cl^- type in the downstream side at both the flow paths. That means the concentration of Cl^- decreases from 560 to 420 mg/L at the first flow path and from 665 to 445 mg/L at the second flow path, while the concentration of HCO_3^- increases from 600 to 855 mg/L at the first flow path and from 590 to 870 at the second flow path (Table 1). Since the present study area is mainly irrigated region, the differences in the concentrations of Cl^- and HCO_3^- ions may be explained by two reasons: First, the irrigation increases the groundwater flow rate, taking away the soluble salts, especially Cl^-, as also reported by Li et al. (2016), and second, irrigation water contains high HCO_3^- due to soil CO_2, which weather and dissolve the minerals of the country rocks more effectively (Stallard and Edmond 1983; Stumm and Morgan 1996).

In the case of concentration of Na^+, there is a significant change in its concentration from the upstream to the downstream (469–410 mg/L) at the first flow path and no significant variation (460–461 mg/L) at the second flow path (Table 1). The difference of Na^+ in its concentration may be explained by two factors: First, when the concentration of Cl^- is higher at the upstream side (560 and 665 mg/L), the concentration of Na^+ is also observed to be high (469 and 460 mg/L) at the upstream side of both the flow paths due to their higher solubility. In the case of Na^+ and HCO_3^- ions, their solubility is low compared to the solubility of Na^+ and Cl^-. However, the concentration of HCO_3^- (590–870 mg/L) is more than that of Cl^- (420–665 mg/L) at both the flow paths due to occurrence of soil CO_2. Second, the traveling distance of groundwater appears to play a significant role. For example, the Na^+ has more or less the same concentration from the upstream to the downstream (460–461 mg/L) at the second flow path due to limited dilution, because the traveling distance of flow path is short (about 3 km). At the first flow path, the traveling distance of groundwater is long (about 12 km), indicating a high dilution compared to the second flow path and therefore the Na^+ shows a significant variation in its concentration from the upstream to the downstream (469–410 mg/L).

From the above discussion, it can be said that the distribution of Na^+, HCO_3^- and Cl^- clearly suggests how the natural conditions (mineral weathering and dissolution)

and artificial inputs (irrigation activities) are responsible for the variation of geochemical characteristics of groundwater along the flow path.

Controlling processes of groundwater chemistry

To further refine the chemical interpretation of geogenic processes (rock weathering, mineral dissolution, ion exchange and evaporation) and anthropogenic sources (irrigation return flow, agrochemicals, wastewaters and constructional activities) as a source of dissolved contents in the groundwater, the various binary diagrams, correlation coefficients and saturation indices of the chemical data of the groundwater of the study area are used.

Geogenic origin

In a plot of Na^+ versus Cl^- (Fig. 7a), all groundwater sampling points fall below the theoretical line (1:1). This suggests that the groundwater has an excess concentration of Na^+ over Cl^-, which derives mainly from the rock weathering (Meyback 1987). If it is so, the groundwater would have HCO_3^- as the dominant ion (Rogers 1989). In 80% of the total groundwater samples, HCO_3^- is observed to be a dominant ion in the present study area (Table 2). The value of pCO_2 is computed (Table 3) on the basis of mean values of pH and HCO_3^- (Eq. 8), following the procedure of Raymahashay (1988). The computed value of pCO_2 is $10^{-2.04}$ atmosphere (atm), which is higher than that of the atmospheric CO_2 ($10^{-3.5}$ atm). It indicates that the groundwater system is open to soil CO_2. During the infiltration of recharge water, it absorbs a large amount of soil CO_2 that is a result of decay of organic matter and root respiration, which in turn combines with rainwater (H_2O) to form HCO_3^- (Eqs. 9 and 10).

$$\log P_{co_2} = 7.82 + \log mHCO_3^- - \text{pH} \quad (8)$$

$$CO_2 + H_2O \rightarrow H_2CO_3 \quad (9)$$

$$H_2CO_3 \rightarrow H^+ + HCO_3^- \quad (10)$$

To further examine the geogenic process, the HCO_3^- is plotted against the concentration of total cations (TC; Fig. 7b). If the dissolution of silicate minerals is a major process controlling the ionic concentration of groundwater, the ratio HCO_3^-: TC would be one (Kim 2003). As shown in Fig. 7b, the groundwater sampling points of the present study area are observed above the equiline (I:I). The deviation of the sampling points from the uniline (I:I) may be caused by the influence of anthropogenic sources as a secondary process over the primary process of rock weathering and mineral dissolution on the groundwater system. Otherwise, the groundwater sampling points must be on the theoretical line of HCO_3^-: TC.

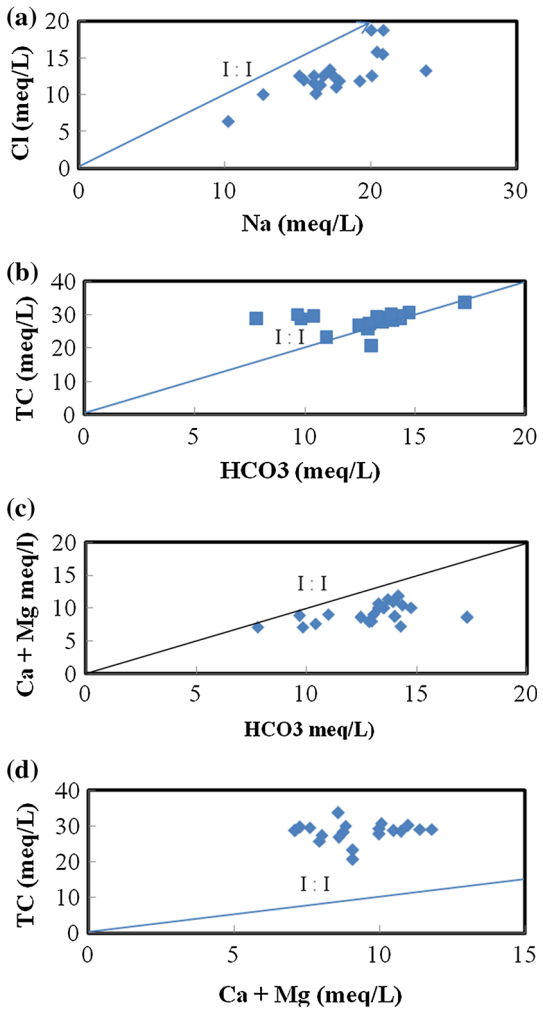

Fig. 7 Relationship between **a** Na^+ and Cl^-, **b** HCO_3^- and TC, **c** $Ca^{2+} + Mg^{2+}$ and HCO_3^- and **d** $Ca^{2+} + Mg^{2+}$ and TC

Table 3 Particulars of pCO_2, Mg^{2+}: Ca^{2+} and Na^+: Ca^{2+}

Particulars	Mean value
pCO_2	$10^{-2.04}$
Mg^{2+}: Ca^{2+}	1.70
Na^+: Ca^{2+}	5.17

The plot of Ca^{2+}+Mg^{2+} versus HCO_3^- is also used to explain the role of silicate weathering as a prime mechanism to release of Na^+ and HCO_3^- ions into the groundwater system. In Fig. 7c, the groundwater sampling points fall below the theoretical line of Ca^{2+}+Mg^{2+}: HCO_3^-. This infers that the groundwater has an excess of HCO_3^- ion, which has been balanced by Na^+. That's why, the groundwater sampling points lie below the equiline of Ca^{2+}+Mg^{2+}: TC (Fig. 7d), which represents an increasing contribution of Na^+ to the major ions caused by silicate weathering. In a plot of Na^+ versus TC (Fig. 8a), the chemical data fall below the equiline, indicating that the supply of cations via silicate weathering and/or soil salts is

more significant (Stallard and Edmond 1983), which also supports the water–rock interactions.

It is also important to note that the high concentration of Na^+ in the groundwater compared to that of other cations (Table 1) is an index of ion exchange process. Figure 8b shows the ion exchange reactions, where Na^+ is plotted against Ca^{2+}, in which Ca^{2+} levels are in between 2 and 5 meq/L and Na^+ levels in between 10 and 25 meq/L. It causes the increase in Na^+ replacing the Ca^{2+} by ion exchange process. If the ion exchange is the only controlling process of groundwater chemistry, the relation between $Ca^{2+}+Mg^{2+}–SO_4^{2-}+HCO_3^-$ and $Na^+–Cl^-$ should have a negative linear trend, as pointed out by Fisher and Mullican (1997), Subba Rao (2008) and Li et al. (2016). In Fig. 8c, the groundwater sampling points show a negative trend of $Ca^{2+}+Mg^{2+}–SO_4^{2-}+HCO_3^-$ versus $Na^+ – Cl^-$ (Eq. 11). However, they spread above and below the linear trend line. Therefore, the controlling of chemical composition of groundwater depends not only on ion exchange process, but also on other process. Otherwise, the spreading of water sampling points above and below the linear trend should not be expected.

$$Y = -1.075x - 1.157;\ r = 0.872 \quad (11)$$

Since the present study area comes under a semiarid climatic region, it leads to a higher rate of evaporation. The groundwater levels are below the depth of 3–5 m from the ground surface, which influences the groundwater chemistry. Such climatic condition is a well-known effective indicator for further enrichment of dissolved ions in groundwater. To examine such phenomena, the groundwater sampling points are plotted in a Na^+: Cl^- versus EC diagram (Fig. 8d), which are spread horizontally. That means that the ratio Na^+: Cl^- does not change with the increase in EC. Therefore, the process of evaporation, as stated by Jankowski and Acworth (1997) and Subba Rao (2008), may be caused by the increase in Na^+ and Cl^- concentrations in the groundwater. This may be true in case of the high evaporation of irrigation water.

The saturation index (SI) is computed with respect to solid phases of calcite ($CaCO_3$), fluorite (CaF_2), halite (NaCl) and gypsum ($CaSO_4$). A positive SI of $CaCO_3$ (0.196–1.629) indicates an oversaturated (precipitated) state (Fig. 9). The occurrence of kankar ($CaCO_3$ concretion) in the soil zone of the present study area supports this hypothesis, which infers a long history of evaporation (Datta and Tyagi 1996). The precipitation of $CaCO_3$ declines Ca^{2+}, which supports a higher concentration of Na^+ in the groundwater. Consequently, the ratio Mg^{2+}: Ca^{2+} is observed to be more than one (1.70) in the groundwater (Table 3). According to Yousaf et al. (1987), where the Na^+ is higher, the Mg^{2+} should be more than Ca^{2+} due to increase in clayey soil dispersion, as in the present study area. Further, the precipitation of $CaCO_3$ can also cause the lower concentration of HCO_3^-, where the enough concentrations of Ca^{2+} and HCO_3^- ions are not reached to the saturated state or where the groundwater has higher concentration of Cl^- than that of HCO_3^- due to interference of human activities on the groundwater system. Hence, the groundwater shows Na^+ and Cl^- as dominant ions in 20% of the total water samples (Table 2). Generally, the solubility of Na^+ and Cl^- is high (Hem 1991). The SI of NaCl is, thus, observed to be negative (− 1.794 to − 5.894) in the groundwater, which indicates unsaturated (dissolved) state (Fig. 10). This supports the higher concentrations of Na^+ (mean 402.55 mg/L) and Cl^- (mean 450.50 mg/L) in the groundwater (Table 1).

It is also observed that the groundwater shows unsaturated state (SI: − 0.623 to − 2.421) with respect to solid phase of $CaSO_4$ (Fig. 10). So, the Ca^{2+} and SO_4^{2-} ions are in the unsaturated (dissolved) state. In the case of $CaCO_3$

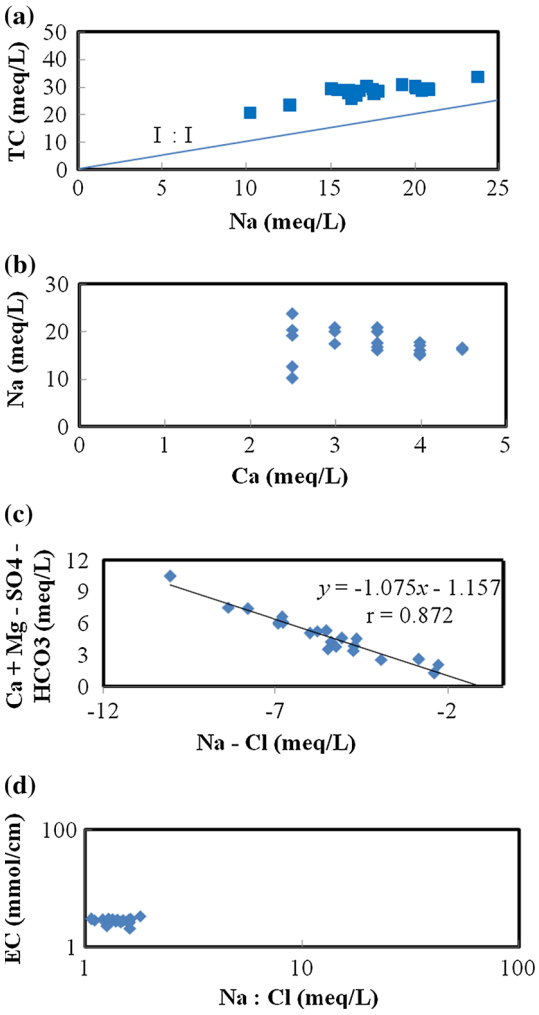

Fig. 8 Relationship between **a** Na^+ and TC^-, **b** Na^+ and Ca^{2+}, **c** $Ca^{2+} + Mg^{2+}–SO_4^{2-} + HCO_3^-$ and $Na^+–Cl^-$ and **d** Na^+: Cl^- and EC

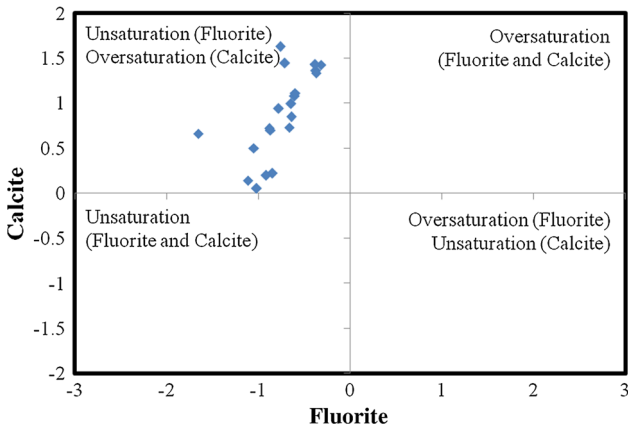

Fig. 9 Saturation index (fluorite and calcite)

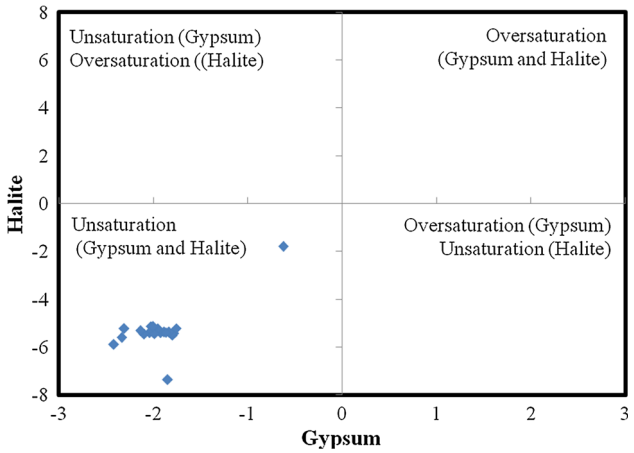

Fig. 10 Saturation index (halite and gypsum)

saturation, the Ca^{2+} and HCO_3^- are in the saturated (precipitated) state (Fig. 9). The contrary situation of Ca^{2+} can be explained by the common ion effect (Freeze and Cherry 1979). According to this effect, the dissolution of $CaSO_4$ causes a decrease in the activity coefficient product ${}_{\Upsilon}Ca^{2+}\cdot{}_{\Upsilon}CO_3^{2-}$. But, the product $(Ca^{2+})(CO_3^{2-})$ increases by a much higher amount due to contribution of Ca^{2+} from the dissolution of $CaSO_4$. By this reason, for the solution to remain in equilibrium with respect to solid phase of $CaCO_3$, precipitation of $CaCO_3$ could occur. Hence, the groundwater shows low concentration of Ca^{2+} (mean 68 mg/L) and high concentration of SO_4^{2-} (mean 90.40 mg/L; Table 1).

Anthropogenic origin

Interpretation of variations in the chemical composition of groundwater due to interference of human activities is a complex process. For instance, irrigation return flow is a source of Ca^{2+}, Mg^{2+}, Na^+, HCO_3^-, Cl^- and SO_4^{2-} in groundwater of the arid and semiarid regions (Todd 1980; Subba Rao et al. 2012a, b; Li et al. 2016). The ions, Mg^{2+}, Na^+, K^+, Cl^-, SO_4^{2-}, NO_3^- and F^-, are widely recognized as contaminants from the application of agrochemicals (nitrogen, phosphate and potash fertilizers), domestic waters and leakage of septic tanks (Todd 1980; Subba Rao et al. 2012a; Li et al. 2016). The lime [Ca (OH_2)] used in cement, which is a part of constructional activities, is the source of Ca^{2+} in groundwater (Somasundaram et al. 1993; Subba Rao et al. 2005; Jiang et al. 2009). These factors enhance the concentrations of chemical composition of groundwater formed by geogenic origin.

The present study area is traditionally agricultural rural region. Sanitary facilities are poor. Constructional activities are not uncommon. Therefore, the anthropogenic inputs including chemical fertilizers, irrigation return flow, wastewater effluents and constructional activities can regulate the chemistry of groundwater. Since all chemical variables contribute to TDS, the studies related to TDS with other ions can be taken into account to explain the impact of human activities on groundwater system. The positive correlation of TDS with Mg^{2+} ($r = 0.24$), Na^+ ($r = 0.63$), K^+ ($r = 0.25$), HCO_3^- ($r = 0.51$), Cl^- ($r = 0.35$), SO_4^{2-} ($r = 0.47$), NO_3^- ($r = 0.28$) and F^- ($r = 0.49$; Table 4) supports the impacts of anthropogenic inputs, in addition to geogenic origin on the groundwater system.

Differences in the values of correlation coefficients among the chemical variables with TDS may be due to variations in the availability of source material and their dissolved capacity along the flow path. Similar observations have been reported in South Korea (Choi et al. 2005), Iran (Jalali 2009), India (Marghade et al. 2012) and China (Li et al. 2016). Another important point to be noted is that an insignificant positive correlation is observed between TDS and Ca^{2+} ($r = 0.08$), because the residential area is limited areal extent in the present study area (Fig. 1). Since the impact of constructional activities is limited on a regional scale, no significant results from the correlation coefficient come out. Otherwise, the relation between TDS and Ca^{2+} should be the similar to the correlation coefficients of others, which have the relations with TDS.

Principal component analysis

The principal component analysis (PCA) is used here in terms of principal component (PC) loadings and PC scores to avoid the confusion over the relative influencing factors in terms of chemical variables on the groundwater system. The PC loadings measure a spatial similarity between the variables and each principal component, while the PC

Table 4 Correlation matrix

	pH	TDS	Ca^{2+}	Mg^{2+}	Na^{+}	K^{+}	HCO_3^{-}	Cl^{-}	SO_4^{2-}	NO_3^{-}	F^{-}
pH	1.00	0.41	0.10	0.52	− 0.11	**0.75**	**0.82**	− 0.40	− 0.12	**0.85**	**0.62**
TDS		1.00	0.08	0.24	**0.63**	0.25	**0.51**	0.35	0.47	0.28	0.49
Ca^{2+}			1.00	− 0.19	− 0.17	0.40	0.08	− 0.04	0.08	0.21	− 0.26
Mg^{2+}				1.00	− 0.39	0.36	0.46	− 0.26	0.15	0.40	0.13
Na^{+}					1.00	− 0.33	− 0.05	**0.74**	0.31	− 0.26	0.43
K^{+}						1.00	0.56	− 0.41	0.03	**0.85**	0.04
HCO_3^{-}							1.00	− 0.54	− 0.01	**0.70**	**0.58**
Cl^{-}								1.00	0.26	− 0.51	− 0.01
SO_4^{2-}									1.00	0.01	− 0.18
NO_3^{-}										1.00	0.32
F^{-}											1.00

Number in bold denotes the high correlation coefficient

scores evaluate the similarity between the observed pattern for a given data and each principal component. The PC scores explain the intensity of the hydrogeochemical processes described by the principal components. Negative PC scores indicate the areas, which are essentially unaffected by the processes. High positive PC scores, which are specified the areas, which are mostly affected by the processes. Near-zero PC scores show the areas, which are affected to an average degree by the processes (Subba Rao et al. 2006).

Principal component loadings

The chemical variables for PCA used in the present study are pH, TDS, Ca^{2+}, Mg^{2+}, Na^{+}, K^{+}, HCO_3^{-}, Cl^{-}, SO_4^{2-}, NO_3^{-} and F^{-} (Table 5). Four principal components (PCs), having eigenvalues higher than one (1.145–4.370), are extracted (Fig. 11), following the procedures of Kaiser's criterion. They account for 87.273% of the total variance of the chemical composition of groundwater with a variation of 39.179–10.421 from PC I to PC IV. The differences in PC loadings indicate the involvement of different contributions in determining the groundwater chemistry.

PC I accounts for 39.179% of the total variance of groundwater chemistry with high loadings of pH (0.967), HCO_3^{-} (0.910), NO_3^{-} (0.887), K^{+} (0.763), Mg^{2+} (0.519) and F^{-} (0.590; Table 5). As pointed out earlier, the occurrence of soil CO_2 combing with rainwater (H_2O) to form HCO_3^{-} (Eqs. 8 and 9) controls the pH (Jacks 1973). The higher HCO_3^{-} in the groundwater (782.50 mg/L; Table 1) infers a dominance of mineral dissolution (Stumm and Morgan 1996). Since there is no known lithological source of NO_3^{-} in the present study area, the substantial contribution of NO_3^{-} (> 10 mg/L) could be mainly result from the application of nitrogen fertilizers for higher crop yields, and also from the domestic effluents and leakage of septic tanks (Cushing et al. 1973; Todd 1980). The K^{+} content comes from the weathering of orthoclase feldspars

Table 5 Principal component loadings

Chemical variables	Principal component loadings			
	I	II	III	IV
pH	**0.967**	0.027	− 0.034	− 0.044
TDS	0.463	**0.728**	0.027	0.417
Ca^{2+}	0.121	− 0.051	**0.910**	0.046
Mg^{2+}	**0.519**	− 0.322	− 0.438	**0.526**
Na^{+}	− 0.142	**0.969**	− 0.061	0.025
K^{+}	**0.763**	− 0.232	0.439	0.170
HCO_3^{-}	**0.910**	0.062	− 0.088	0.011
Cl^{-}	− 0.499	**0.701**	0.036	0.200
SO_4^{2-}	− 0.071	0.272	0.108	**0.861**
NO_3^{-}	**0.887**	− 0.162	0.205	0.063
F^{-}	**0.590**	**0.554**	− 0.379	− 0.345
Eigenvalue	4.310	2.612	1.532	1.146
% of total variance	39.179	23.745	13.928	10.421
% cumulative variance	39.179	62.924	76.852	87.273

Number in bold denotes the high positive loading

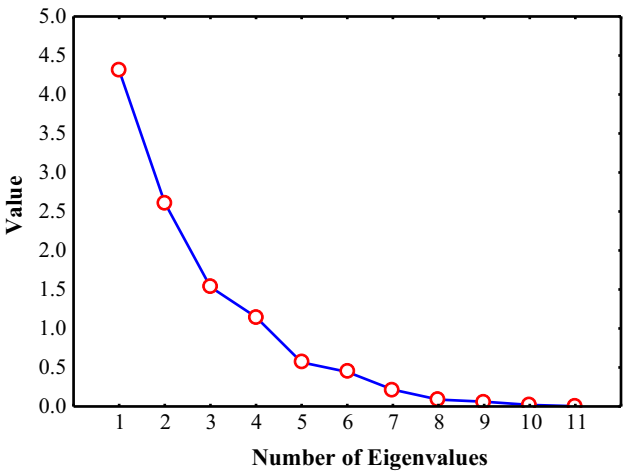

Fig. 11 Plot of eigenvalues

present in the country rocks and also from the surface pollution caused by potash fertilizers. As explained earlier, 70% of the total groundwater samples have the K^+ as the additional ion in cation facies in the study area (Table 2), which is also supported by the anthropogenic pollution (potash fertilizers). The Mg^{2+} derives mainly from the weathering of ferromagnesium minerals of the country rocks and also from the wastewater effluents (Todd 1980; Hem 1991). The dissolution of F^--bearing minerals (hornblende, biotite and apatite) present in the country rocks are the main source of F^- in the groundwater (Eqs. 12–14), which are more active under alkaline (HCO_3^-) condition (Subba Rao et al. 2013; Jabal et al. 2014; Rao et al. 2014; Reddy et al. 2016). The usage of phosphate fertilizers and the anion exchange between F^- and OH^- due to occurrence of clays also causes an enrichment of F^- in groundwater (Robinson and Edington 1946; Ayoob and Gupta 2006; Ahmed 2014; Subba Rao et al. 2013). This is also supported by the dominance of HCO_3^- (mean 782.50 mg/L) compared to other ions in the study area (Table 1). As shown in Table 4, there are significant positive correlations between pH and Mg^{2+} ($r = 0.52$), pH and HCO_3^- ($r = 0.82$), pH and F^- ($r = 0.62$), HCO_3^- and F^- ($r = 0.58$), HCO_3^- and Mg^{2+} ($r = 0.46$) and K^+ and NO_3^- ($r = 0.85$). These relations clearly support the rock weathering, mineral dissolution and agrochemicals (nitrogen, phosphate and potash fertilizers) rather than that of domestic effluents and leakage of septic tanks on the groundwater system. Therefore, the high loadings of chemical variables (pH, HCO_3^-, NO_3^-, K^+, Mg^{2+} and F^-) in PC1 are related to mineral weathering and dissolution, and agrochemicals.

$$KMg_3(AlSi_3O_{10})F_2 + 2OH^- \rightarrow KMg_3(AlSi_3O_{10})(OH^-)_2 + 2F^-$$

Biotite (12)

$$(Ca, Na)_{2-3}(Mg, Fe, Al)_5(Al, Si)_8O_{22}(OH, F) \rightarrow (Ca, Na)_{2-3}(Mg, Fe, Al)_5(Al, Si)_8O_{22}(OH)_2 + 2F^-$$

Hornblende (13)

$$Ca_5(PO_4)_3(F, Cl, OH) \rightarrow Ca_5(PO_4)_3(Cl, OH) + F^-$$

Apatite (14)

PC II, accounting for 23.745% of the total variance in the chemistry of groundwater, consists of Na^+ (0.969), TDS (0.728), Cl^- (0.701) and F^- (0.554; Table 5). The TDS measures the total amount of dissolved ions in the groundwater, causing salinity in the groundwater. The geogenic and non-geogenic origins are the sources of salinity. For example, Na^+ derives mainly from the incongruent dissolution of plagioclase feldspars present in the country rocks (Eq. 15), irrigation return flow, drainage effluents and leakage of septic tanks (Todd 1980; Stallard and Edmond 1983). Further, the increase in Na^+ relative to Ca^{2+} is caused by ion exchange (Fig. 6b) and also precipitation of $CaCO_3$ (SI: 0.196–1.629; Fig. 9) due to evaporation. Chloride has a non-lithological source and is derived mainly from the secondary salt precipitation due to irrigation return flow, higher rate of evaporation due to semiarid climate, and pollution of sewage wastes and leakage of septic tanks (Todd 1980; Hem 1991). However, the Cl^- ion also derives from the clay weathering products due to their poor drainage conditions (Hem 1991). Fluoride is caused by clays and F^--rich minerals identified in the country rocks and the application of phosphate fertilizers. Further, the solubility of Na^+ and Cl^- ions is high (Hem 1991). Therefore, the SI of NaCl is observed to be − 1.794 to − 5.894, indicating the unsaturated (dissolved) state of Na^+ and Cl^- ions in the groundwater (Fig. 10). These two ions enhance the value of TDS, which increases the ionic strength (0.023–0.038; Fig. 12). This increases the solubility of CaF_2 (Rogers 1989), causing the higher F^- content in the groundwater (Eq. 16; Fig. 9). The Na^+ also favors the release of F^- (Apambire et al. 1997). From Table 4, it is observed that there are positive correlations between Na^+ and TDS ($r = 0.63$), Cl^- and TDS ($r = 0.35$), Na^+ and Cl^- ($r = 0.74$), Na^+ and F^- ($r = 0.43$) and F^- and TDS ($r = 0.49$). These correlations also support the above views. Therefore, PC II is mainly related to the mineral weathering and dissolution, ion exchange, evaporation, irrigation return flow and phosphate fertilizers.

$$2Na^+[AlSi_3O_8 + 2CO_2]^- + 11H_2O \rightarrow 2Na^+ + 2HCO_3^- + Al_2Si_2O_5(OH)_4 + Mg^{2+} + 4H_4SiO_4$$

Plagioclase feldspar (15)

$$CaF_2 + 2HCO_3^- \rightarrow CaCO_3 + H_2O + CO_2 + 2F^-$$

Fluorite (16)

PC III has high loading of Ca^{2+} (0.910) with an account of 13.928% of the total variation of groundwater chemistry (Table 5). Calcium derives mainly from the dissolution of calcium feldspars to the groundwater (Hem 1991). The application of amendments (gypsum) to alter the physical and chemical properties of soils and the constructional activities may be the additional source of Ca^{2+} to the existing groundwater quality, as also reported by Todd (1980), Somasundaram et al. (1993), Subba Rao et al. (2005) and Jiang et al. (2009). Therefore, PC III is considered as a result of mineral weathering and dissolution, and constructional activities.

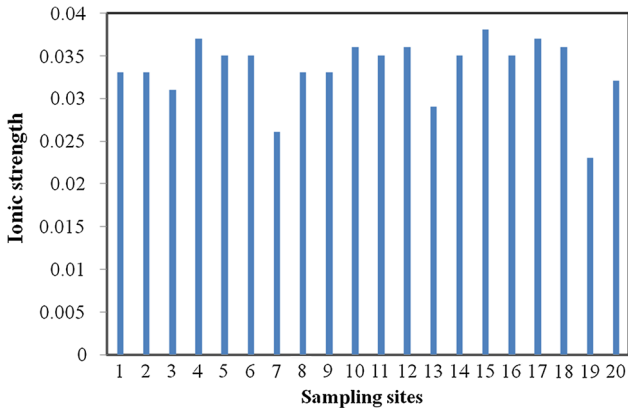

Fig. 12 Sampling sites versus ionic strength

PC IV accounts for 10.421% of the total variance in the chemical composition of groundwater, consisting of SO_4^{2-} (0.861) and Mg^{2+} (0.526; Table 5). Since, there is no lithological source of SO_4^{2-} in the present study area, it comes from the sources of soil amendments (gypsum) used to improve the soil permeability (Todd 1980). As mentioned earlier, 75% of the total groundwater samples have the SO_4^{2-} as the additional ion in their anion facies in the study area (Table 2). This occurrence is also supported by the impact of anthropogenic pollution on the groundwater body. The sources of Mg^{2+} include ferromagnesium minerals present in the country rocks and domestic waters (Todd 1980; Hem 1991). The low positive correlation is noticed between Mg^{2+} and SO_4^{2-} ($r = 0.15$; Table 4). This suggests that the sources of these ions are different. Therefore, PC IV is assumed to be indicative of mineral weathering and dissolution, and soil amendments.

Principal component scores

In order to highlight the specific effects of geogenic processes (water–rock interaction, ion exchange and evaporation) and non-geogenic activities (chemical fertilizers, irrigation return flow, wastewaters and constructional activities) on a regional scale of the aquifer system, the high positive PC scores are intended to be > 1 and their locations are shown in Fig. 13. This gives the information on relative impact of factors in each sampling site.

The high positive scores of PC I (1.052–1.894; Table 6) are observed from the northeastern (sample 12), western (sample 10), central (sample 15) and southeastern (sample 14) sectors (Fig. 13). They show the high pH (8.48), Mg^{2+} (77.75 mg/L), K^+ (78.50 mg/L), HCO_3^- (906.25 mg/L), NO_3^- (72.75 mg/L) and F^- (5.30 mg/L) compared to those of the respective chemical variables of the negative and low positive scores (Table 7). This clearly suggests that PC I is mainly associated with the mineral weathering and dissolution, and agrochemicals (nitrogen, phosphate and potash varieties), which is further supported the hypothesis of the effects on the chemical variables (pH, HCO_3^-, NO_3^-, K^+, Cl^-, Mg^{2+} and F^-) as explained in the earlier in PC I loadings.

Two locations show the high positive scores of PC II (1.025–2.474), which are in the central (sample 15) and southeastern (sample 16) sectors of the study area (Table 6 and Fig. 13). There is a gradual increase in TDS (1792.08–2080 mg/L), Na^+ (371.42–503 mg/L), Cl^- (400.83–567.50 m/L) and F^- (1.84–7.15 mg/L) from the negative and low positive scores (Table 7). This obviously indicates that the higher F^- could be due to TDS and Na^+ in the groundwater. Thus, this also supports the hypothesis of the effect of mineral weathering and dissolution, ion exchange, evaporation, irrigation return flow and phosphate fertilizers on the chemicals (Na^+, TDS, Cl^- and F^-) as clarified in the previous section of PC II loadings.

The high positive scores of PC III (1.524–1.681) are observed from the northeastern (sample 3) and southeastern (sample 20) sectors (Table 6 and Fig. 13). They show the high concentration of Ca^{2+} (90 mg/L) compared to that in the negative (57.50 mg/L) and low positive (71.11 mg/L) scores (Table 7). The precipitation of $CaCO_3$ supported by the occurrence of $CaCO_3$ concretions (kankar) in the soils due to semiarid climate in the study area and the higher ratio of Na^+: Ca^{2+} (5.17; Table 3) reduce the concentration of Ca^{2+} in the groundwater. However, if the controlling factor is uniform on the groundwater system, the contribution of Ca^{2+} should be the same in the entire study area on a regional scale. But, it is not so. That means the contribution of Ca^{2+} may be totally local phenomena on the groundwater system. Thus, the additional concentration of Ca^{2+} in PC III scores compared to that of the negative and low positive scores could be due to constructional activities.

The PC IV shows the high positive scores (1.070–1.981), which are observed from the northeastern (samples 5 and 12), central (sample 4) and southeastern (sample 18) sectors (Table 6 and Fig. 13). They have the higher concentrations of Mg^{2+} (88.75 mg/L) and SO_4^{2-} (134.50 mg/L) relative to those of the negative (Mg^{2+}: 61.40 mg/L and SO_4^{2-}: 69.50 mg/L) and positive (Mg^{2+}: 72.67 mg/L and SO_4^{2-}: 95.83 mg/L) scores (Table 7). Thus, the mineral weathering and dissolution, and soil amendments could be the main sources of Mg^{2+} and SO_4^{2-} on the groundwater system, as stated in the earlier section of PC IV loadings.

Finally, the above discussion suggests that the geogenic processes are the natural sources (primary) to control the groundwater chemistry. The others, which are related to the human activities, are the artificial sources (secondary) responsible for modifications of the existing chemistry of groundwater. Therefore, the chemical composition of

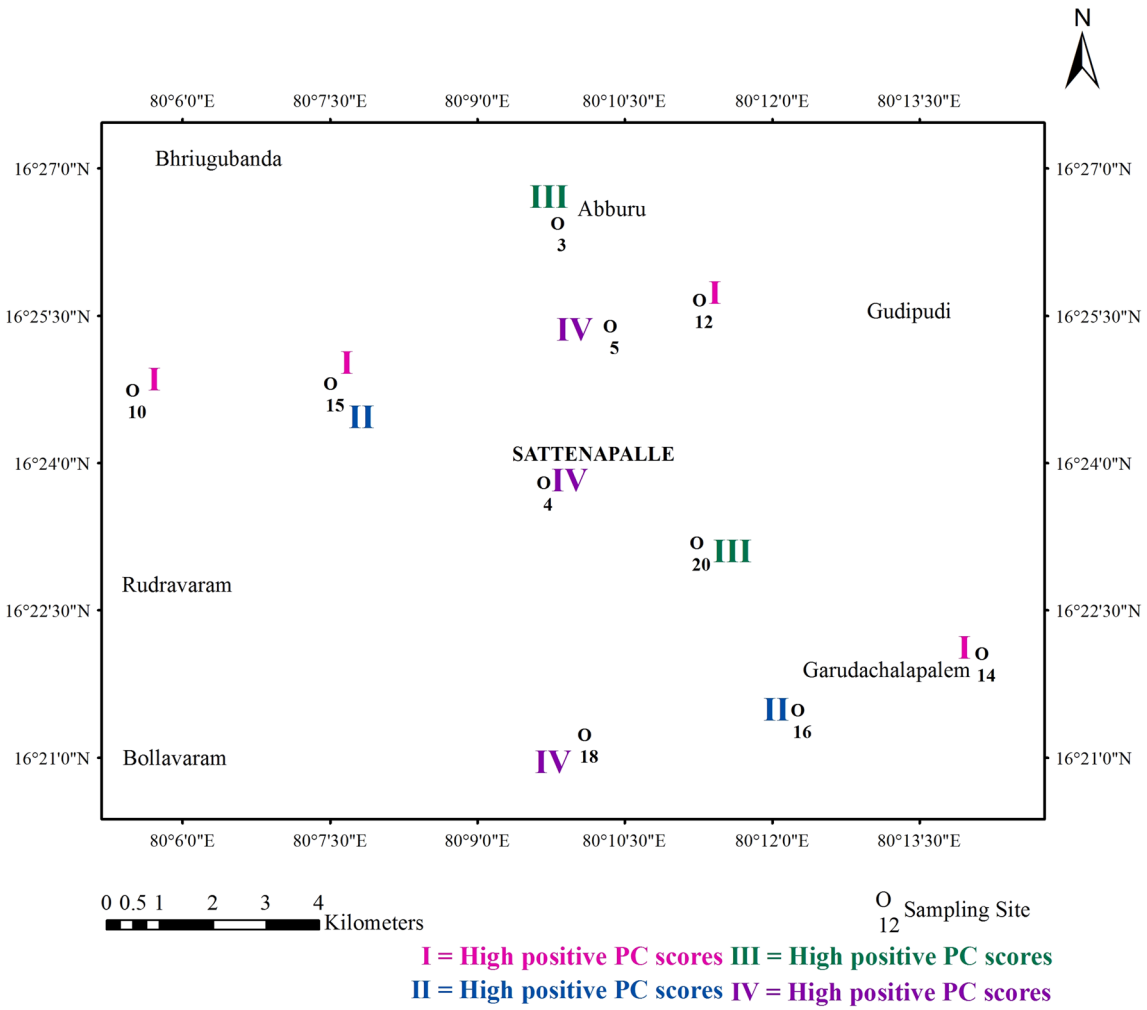

Fig. 13 High positive principal component scores with sampling sites

groundwater controlled by geogenic origin is subsequently modified by non-geogenic origin.

Geochemical modeling of groundwater

The hydrogeochemical facies, trilinear graphic analysis, ionic plots, correlation coefficients, saturation indices and principal component analysis show that the chemical composition of groundwater is mainly controlled by geogenic origin, which is subsequently modified by non-geogenic origin. Geochemical modeling of groundwater is also used in this study to support the findings. It is performed with PHREEQC (Parkhurst and Appelo 1999).

On basis of geochemical findings, the following minerals are considered as the possible mineral phases for geochemical modeling: calcite, dolomite, fluorite, halite, gypsum, K-feldspar and albite. As the ion exchange is responsible for the increase in Na^+ relative to Ca^{2+}, the precipitation of $CaCO_3$ is included in modeling. Carbon dioxide is considered for the simulation as the recharge water infiltrates through the soil zone and finally become groundwater. The simulation is carried on the first flow path from 8 to 2 and the second flow path from 16 to 14 along which groundwater chemistry changes from Na^+–Cl^- to Na^+ –HCO_3^- types. The mole transfer of phases calculated by PHREEQC is listed in Table 8.

From the geochemical modeling of the groundwater, it is observed that the dissolution of gypsum, anhydrite, calcite, dolomite, K-feldspar and CO_2 took place along the first simulated path. At the same time, cation exchange between Na^+ and Ca^{2+} occurred (Li et al. 2010). It is found that the cation exchange increases the concentration of Na^+, but the precipitation of albite lowers its concentration. Due to the long traveling distance of the first flow path (about 8 km), a high dilution affect the concentration of Na^+ from the upstream to the downstream. In this flow path, hydrochemical type changes from Na^+–Cl^-–HCO_3^- to Na^+–HCO_3^-–Cl^- from the upstream to the downstream. As mentioned above, the decrease in concentration of Cl^- observed along the first flow path may be due to continuous

Table 6 Principal component scores

Sample numbers	Principal component scores			
	I	II	III	IV
1	− 2.162	0.567	− 0.334	− 0.774
2	0.008	0.135	0.827	− 0.507
3	− 0.232	− 0.300	**1.681**	− 0.911
4	− 0.107	0.082	− 1.501	**1.981**
5	0.153	− 0.285	− 0.217	**1.574**
6	0.163	− 0.230	− 0.352	0.156
7	− 0.060	− 2.455	− 1.530	− 1.270
8	− 1.547	0.692	− 0.740	0.453
9	0.319	− 0.416	0.588	− 0.664
10	**1.052**	− 0.510	0.484	0.431
11	− 1.117	0.981	0.483	0.556
12	**1.153**	− 0.440	0.761	**1.070**
13	− 0.259	− 1.659	− 1.240	− 0.812
14	**1.063**	0.590	0.689	− 0.881
15	**1.894**	**2.474**	− 1.893	− 1.631
16	− 1.389	**1.025**	0.041	0.090
17	0.935	0.133	0.657	0.868
18	0.578	− 0.112	− 0.364	**1.275**
19	− 0.171	− 0.118	0.437	− 0.444
20	− 0.274	− 0.154	**1.524**	− 0.559

Number in bold denotes the high positive score

irrigation, which increases groundwater flow rate and also HCO_3^- concentration, as a result of soil CO_2 dissolution. The involvement of CO_2 enhances the dissolution of minerals. Further, 70% of the total groundwater samples have the K^+ as the additional ion in cation facies in the study area (Table 2). The K^+ derives mainly from the weathering of K^+-feldspars present in the country rocks and also from the application of potash fertilizers used for higher crop yields. Therefore, a positive value of mineral mass balance is obtained. Overall, the dissolution of calcite, dolomite and gypsum increases Ca^{2+} concentration, whereas cation exchange as well as calcite and anhydrite precipitation decreases Ca^{2+} concentration. According to Li et al. (2010), the dissolved CO_2 caused the water pH value to decrease, promoting the dissolution of gypsum along with cation exchange, increases Ca^{2+} concentration, resulting in precipitation of calcite, dolomite and fluorite. In the study area, a very small amount of CO_2 dissolved due to continuous recharging result in precipitation of fluorite only.

The traveling distance of the second flow path is 3 km long. The simulation model in this flow path shows some small differences from the first flow path, even though the hydrochemical type changes from Na^+–Cl^-–HCO_3^- to Na^+–HCO_3^-–Cl^- from the upstream to the downstream. The dissolution of fluorite increases along the flow path. The halite dissolution is the main process, explaining the increase in the concentrations of Na^+–Cl^- ions in the second flow path, which increase the dissolution of fluorite. The dissolution of gypsum is responsible for the elevation of Ca^{2+} concentration, whereas anhydrite is responsible for precipitation of Ca^{2+}, resulting in low concentration of Ca^{2+} than that of Na^+. These differences in the water–rock interactions occurred between the two flow paths should be attributed to variations in the hydrogeological conditions. Gypsum and dolomite dissolution in the aqueous solution should have caused a noticeable increase in Ca^{2+}. But in the study area, the concentration of Ca^{2+} decreases along the first and second flow paths due to cation exchange.

Table 7 Average concentrations of influential chemical variables in PC scores

Chemical variables	PC1			PC II			PC III			PC IV		
	Negative	Positive		Negative	Positive		Negative	Positive		Negative	Positive	
		Low	High		Low	High		Low	High		Low	High
pH	7.53	8.12	8.48	–	–	–	–	–	–	–	–	–
TDS (mg/L)	–	–	–	1792.08	1857.14	2080.00						
Ca^{2+} (mg/L)	–	–	–	–	–	–	57.50	71.11	90.00	–	–	–
Mg^{2+} (mg/L)	62.00	79.00	77.75		–	–	–	–	–	61.40	72.67	88.75
Na^+ (mg/L)	–	–	–	371.42	447.71	503.00	–	–	–	–	–	–
K^+ (mg/L)	52.00	67.00	78.50	–	–	–	–	–	–	–	–	–
HCO_3^- (mg/L)	700.00	837.50	906.25	–	–	–	–	–	–	–	–	–
Cl^- (mg/L)				400.00	505.00	567.50	–	–	–	–	–	–
SO_4^{2-} (mg/L)	–	–	–	–	–	–	–	–	–	69.50	95.83	134.50
NO_3^- (mg/L)	47.40	59.00	72.75	–	–	–	–	–	–	–	–	–
F^- (mg/L)	1.55	2.03	5.30	2.88	1.84	7.15	–	–	–	–	–	–

Table 8 Mineral transfer amount calculated by PHREEQC (unit: mmol/L)

Phases	Chemical expression	Simulation path	
		First flow path From 8 to 2	Second flow path From 16 to 14
Calcite	$CaCO_3$	0.00325	0.00285
CaX_2	CaX_2	− 0.00457	− 0.00427
Dolomite	$CaMg(CO_3)_2$	0.00244	0.00214
Fluorite	CaF_2	− 0.00005	0.00008
Halite	NaCl	− 0.00113	0.01283
Gypsum	$CaSO_4.2H_2O$	27.7600	27.7600
K-feldspar	$KAlSi_3O_8$	0.00167	0.00228
NaX	NaX	0.00915	0.00853
Albite	$NaAlSi_3O_8$	− 0.00167	− 0.00228
Anhydrite	$CaSO_4$	27.76000	− 27.7600
$CO_2(g)$	CO_2	0.00827	0.00668

Therefore, the geochemical modeling of groundwater (first and second flow paths) shows that water–rock interactions are the governing factors responsible for the chemical composition of groundwater. However, the rate of reaction and intensity are influenced by dry climate and man-made activities, as also reported by Li et al. (2016).

Conclusions

Groundwater is an important source for various purposes in the developing countries. The hydrogeochemical facies, graphical approaches, binary diagrams, correlation coefficients, saturation indices, principal component analysis and geochemical modeling of groundwater were applied to assess the geochemical characteristics and controlling factors of groundwater. The following conclusions were drawn from the study area:

- Groundwater chemistry is of alkaline nature.
- Five hydrogeochemical facies, (a) $Na^+ > Mg^{2+} > Ca^{2+} > K^+$: $HCO_3^- > Cl^- > SO_4^{2-}$, (b) $Na^+ > Mg^{2+} > Ca^{2+}$: $HCO_3^- > Cl^- > SO_4^{2-}$, (c) $Na^+ > Mg^{2+} > Ca^{2+} > K^+$: $HCO_3^- > Cl^-$, (d) $Na^+ > Mg^{2+} > Ca^{2+}$: $Cl^- > HCO_3^- > SO_4^{2-}$ and (e) $Na^+ > Mg^{2+} > Ca^{2+}$: $HCO_3^- > Cl^-$, are observed to be dominant in 5, 5, 20, 50 and 20% of the total groundwater samples.
- Along the specific flow paths, the concentration of Cl^- decreases, while the concentration of HCO_3^- increases, as the irrigation increases the groundwater flow rate, taking away the soluble salts, especially Cl^-, and irrigation water contains more HCO_3^- due to a result of soil CO_2.
- As per the trilinear diagram, the mixed water moves toward the saline water due to influence of anthropogenic activity on the groundwater chemistry formed by geogenic origin.
- Binary diagrams, correlation coefficients and saturation indices of the chemical data of the groundwater suggest that the geogenic processes (mineral weathering and dissolution, ion exchange and evaporation) and anthropogenic sources (irrigation return flow, agrochemicals, domestic wastes, leakage of septic tanks and constructional activities) are the dominant factors to control the chemical composition of groundwater.
- Four PCs are extracted from PCA, accounting 87% of the total variance of the groundwater quality. The loadings of PC I are high positive for pH, HCO_3^-, NO_3^-, K^+, Mg^{2+} and F^-, representing the rock weathering, mineral dissolution and agrochemicals (nitrogen, phosphate and potash fertilizers).
- The loadings observed from PC II are highly positive for Na^+, TDS, Cl^- and F^-, which are associated with the mineral weathering and dissolution, irrigation return flow and phosphate fertilizers.
- The PC III has high loading of Ca^{2+} due to the impact of constructional activity, while the PC IV shows high positive loading of Mg^{2+} and SO_4^{2-}, attributing the mineral weathering and dissolution, and soil amendments.
- The spatial distribution of PC scores elucidate that the geogenic processes are the primary sources, and the anthropogenic activities are the secondary sources to enrich the chemical composition of groundwater.
- The geochemical modeling of groundwater supports the water–rock interactions, which are assessed with respect to the phases of calcite, dolomite, fluorite, halite, gypsum, K-feldspar, albite and CO_2. The water–rock interactions are, thus, the main factors regulating the chemistry of groundwater. However, the rate of

reaction and intensity are further influenced by climate and human activities.

- The study will be helpful in the protection of groundwater quality with suitable remedial measures, according to the controlling factors of chemical composition of groundwater.

Acknowledgements The authors are thankful to the editor and anonymous reviewers for their valuable suggestions and useful comments to improve the quality of the paper.

References

Ahmed AA (2014) Fluoride in quaternary groundwater aquifer, Nile Valley, Luxor, Egypt. Arab J Geosci 7:3069–3083

Apambire WB, Boyle DR, Michel FA (1997) Geochemistry, genesis and health implications of fluoriferous groundwaters in the upper regions of Ghanna. Environ Geol 33:13–24

APHA (1992) Standard methods for the examination of water and wastewater. American Public Health Association, Washington

Ayoob S, Gupta AK (2006) Fluoride in drinking water: a review on the status and stress effects. Crit Rev Environ Sci Technol 36:433–487

Back W (1966) Hydrochemical facies and groundwater flow pattern in Northern Part of Atlantic Coastal Plain. US Geol Surv Paper 498A:42

BIS (2012) Indian standard specifications for drinking water. IS:10500, Bureau of Indian Standards, New Delhi

CGWB (2013) Groundwater Brochure, Guntur district, Andhra Pradesh, India. Central Ground Water Board, Ministry of Water resources, Government of India

Choi BY, Yun ST, Yu SY, Lee PK, Park SS, Chae GT (2005) Hydrochemistry of urban groundwater in Seoul, South Korea: effect of land use and pollutant recharge. Environ Geol 48:979–990

Cushing EM, Kantrowitz IH, Taylor KR (1973) Water resources of the Delmarva Peninsular. U. S. Geological Survey Professional Paper 822, Washington DC, p 58

Dalton MG, Upchurch SB (1978) Interpretation of hydrochemical facies by factor analysis. Ground Water 16:228–233

Datta PS, Tyagi SK (1996) Major ion chemistry of groundwater in Delhi area: chemical weathering processes and groundwater flow regime. J Geol Soc India 47:179–188

Davis JC (1986) Statistics and data analysis in geology. Wiley, New York

Domenico PA, Schwartz FW (1990) Physical and chemical hydrogeology. Wiley, New York, p 824

Drever JI (1997) The geochemistry of natural waters. Prentice Hall, Englewood, p 436

Fisher RS, Mullican FW (1997) Hydrochemical evolution of sodium-sulfate and sodium-chloride groundwater beneath the Northern Chihuahuan Desert, TransPecos, Texas, USA. Hydrogeol J 5:14–16

Freeze RA, Cherry JA (1979) Groundwater. Prentice-Hall, New Jersey, p 603

Hem JD (1991) Study and interpretation of the chemical characteristics of natural water; U.S. Geological Survey Water Supply Paper 2254, Scientific Publishers, Jodhpur, India, p 264

Jabal MSA, Abustan I, Rozaimy MR, Al-Najar H (2014) Fluoride enrichment in groundwater of semi-arid urban area: Khan Younis City, southern Gaza Strip (Palestine). J Afr Earth Sci 100:259–266

Jacks G (1973) Chemistry of groundwater in a district of Southern India. J Hydrol 18:185–200

Jalali M (2009) Geochemistry characterisation of groundwater in an agricultural area of Razan, Hamadan, Iran. Environ Geol 56:1479–1488

Jankowski J, Acworth RI (1997) Impact of debris-flow deposits on hydrogeochemical processes and the development of dry land salinity in the Yass River Catchment, New South Wales, Australia. Hydrogeol J 5:71–88

Jiang Y, Wu Y, Groves Ch, Yun D, Kambesis P (2009) Natural and anthropogenic factors affecting the groundwater quality in the Nandong Karst underground river system in Yunan, Vhina. J Contamin Hydrol 109:49–61

Kaiser HF (1958) The varimax criterion for analytic rotation in factor analysis. Psychometrika 23:187–200

Kazi TG, Arain MB, Jamali MK, Jalbani N, Afidir HI, Sarfraz RA, Baig JA, Shah AG (2009) Assessment of water quality of polluted lake using multivariate statistical techniques: a case study. Eco-Toxicol Environ Safe 72:301–309

Khan RA, Ferrell RE, Billings GK (1972) Geochemical hydrology of the Baton Rouge aquifers. Louisiana Water Resources Research Institute, Bull 8, p 63

Kim K (2003) Long-term disturbance of groundwater chemistry following well installation. Ground Water 41:780–789

Kim H, Park S (2016) Hydrogeochemical characteristics of groundwater highly polluted with nitrate in an agricultural area of Hongseong, Korea. Water 8:7–18

Li P-Y, Qian H, Wu J-H, Ding J (2010) Geochemical modeling of groundwater in southern plain area of Pengyang County, Ningxia, China. Water Sci Eng 3(3):282–291

Li P, Wu J, Qian H, Zhang Y, Yang N, Jing L, Yu P (2016) Hydrogeochemical characterization of groundwater in and around a wastewater irrigated forest in the southeastern edge of the Tengger Desert, Northwest China. Expo Health 8:331–348

Mahlknecht J, Steinich B, de Navarro LL (2004) Groundwater chemistry and mass transfers in the independence aquifer, central Mexico by using multivariate statistics and mass balance models. Environ Geol 45:781–795

Marghade D, Malpe DB, Zade AB (2012) Major ion chemistry of shallow groundwater of a fast growing city of Central India. Environ Monit Assess 184:2405–2418

Marghade D, Malpe DB, Subba Rao N (2015) Identification of controlling processes of groundwater quality in a developing urban area using principal component analysis. Environ Earth Sci 74:5919–5933

Meyback M (1987) Global chemical weathering of surficial rocks estimated from river dissolved loads. Am J Sci 287:401–428

Nosrati K, Eeckhaut VN (2012) Assessment of groundwater quality using multivariate statistical techniques in Hashtgerd Plain, Iran. Environ Earth Sci 65:331–344

Parkhurst DL, Appelo CAJ (1999) User's guide to PHREEQC (version 2)—a computer program for speciation, batch-reaction, one-dimensional transport, and inverse geochemical calculations. United States Geological Survey. Water Resources Investigations Report 99-4259, Washington DC

Piper AM (1944) A graphical procedure in the geochemical interpretation of water analysis. Trans Am Geophys Union 25:914–928

Rao PN, Rao AD, Bhargav JS, Siva Sankar K, Sudarshan G (2014) Regional appraisal of the fluoride occurrence in groundwaters of Andhra pradesh. J Geol Soc India 84:483–493

Ravikumar P, Somashekar RK (2017) Principal component analysis and hydrochemical facies characterization to evaluate groundwater quality in Varahi River Basin, Karnataka State, India. Appl Water Sci 7:745–755

Raymahashay BC (1988) Geochemistry for hydrologists. Allied Pub Ltd, New Delhi, p 190

Reddy AGS (2013) Evaluation of hydrogeochemical characteristics of phreatic alluvial aquifers in southeastern coastal belt of Prakasam district, South India. Environ Earth Sci 68:471–485

Reddy AGS, Reddy DV, Kumar MS (2016) Hydrogeochemical processes of fluoride enrichment in Chimakurthy pluton, Prakasam District, Andhra Pradesh, India. Environ Earth Sci 75:663–680

Robinson WD, Edington G (1946) Fluorine in soils. Soil Sci 61:341–353

Rogers RJ (1989) Geochemical comparison of groundwater in areas of New England, New York and Pennsylvania. Ground Water 27:690–712

Sarikhani R, Dehnavi AG, Ahmadnejad Z, Kalantari N (2015) Hydrochemical characteristics and groundwater quality assessment in Bushehr Province, SW Iran. Environ Earth Sci 74:6265–6281

Seaber PR (1962) Cation hydrochemical facies of groundwater in the English town formation, New Jersey. U.S. Geol Surv Prof Paper 450B:124–126

Senthilkumar G, Ramanathan AL, Nainwal HC, Chidambaram S (2008) Evaluation of the hydrogeochemistry of groundwater using factor analysis in the Cuddalore coastal region, Tamilnadu, India. Indian J Mar Sci 37:181–185

SERI (2009) State of Environment Report India (SERI). Ministry of Environment and Forests, Government of India, p 179

Singaraja C, Chidambaram S, Anandhan P, Prasanna MV, Thivya C, Thilagavathi R, Sarathidasan J (2014) Geochemical evaluation of fluoride contamination of groundwater in the Thoothukudi District of Tamilnadu, India. Appl Water Sci 4:241–250

Somasundaram MV, Ravindran G, Tellam JH (1993) Groundwater pollution of the Madras urban aquifer, India. Ground Water 31:4–11

Srinivasamoorthy M, Vasanthavigar S, Chidambaram S, Anandan P, Sharma VS (2011) Characterization of groundwater chemistry in an eastern coastal area of Cuddalore district, Tamilnadu. J Geol Soc India 78:549–558

Stallard RF, Edmond JM (1983) Geochemistry of the Amazon River—the influence of the geology and weathering environment on the dissolved load. J Geophy Res 88:9671–9688

Stumm W, Morgan JJ (1996) Aquatic chemistry. Wiley-Interscience, New York, p 780

Subba Rao N (2002) Geochemistry of groundwater in parts of Guntur District, Andhra Pradesh, India. Environ Geol 41:552–562

Subba Rao N (2008) Factors controlling the salinity in groundwater from a part of Guntur district, Andhra Pradesh, India. Environ Monit Assess 138:327–341

Subba Rao N (2013) Development and management of groundwater resources in a coastal region: a study from Prakasam District, Andhra Pradesh. Presented at 3rd DST PACWTI on 12th January 2013, Andhra University, Visakhapatnam

Subba Rao N (2014) Spatial control of groundwater contamination, using principal component analysis. J Earth Syst Sci 123:715–728

Subba Rao N, Saroja Nirmal I, Suryanarayana K (2005) Groundwater quality in a coastal area—a case study from Andhra Pradesh, India. Environ Geol 48:534–550

Subba Rao N, John Devadas D, Srinivasa Rao KV (2006) Interpretation of groundwater quality using principal component analysis from Anantapur District, Andhra Pradesh, India. Environ Geosci 13:1–21

Subba Rao N, Subrahmanyam A, Ravi Kumar S, Srinivasulu N, Babu Rao G, Surya Rao P, Venktram Reddy G (2012a) Geochemistry and quality of groundwater of Gummanampadu Sub-basin, Guntur District, Andhra Pradesh, India. Environ Earth Sci 67:1451–1471

Subba Rao N, Surya Rao P, Venktram Reddy G, Nagamani M, Vidyasagar G, Satyanarayana NLVV (2012b) Chemical characteristics of groundwater and assessment of groundwater quality in Varaha River Basin, Visakhapatnam District, Andhra Pradesh, India. Environ Monit Assess 184:5189–5214

Subba Rao N, Subrahmanyam A, Babu Rao G (2013) Fluoride-bearing groundwater in Gummanampadu Sub-basin, Guntur District, Andhra Pradesh, India. Environ Earth Sci 70:575–586

Todd DK (1980) Groundwater hydrology. Wiley Publications, New York

Vasanthavigar M, Srinivasamoorthy K, Prasana MV (2013) Identification of groundwater contamination zones and its sources by using multivariate statistical approach in Thirumanimuthat sub-basin, Tamil Nadu, India. Environ Earth Sci 68:1783–1795

WHO (2011) Guidelines for drinking water quality. World Health Organization, Geneva

Yousaf M, Ali OM, Rhoades JD (1987) Dispersion of clay from some salt-affected, and land soil aggregates. Soil Sci Soc Am J 51:920–924